INSTITUT DE FRANCE
Académie des sciences

Comptes Rendus
Mécanique

Paul Clavin

Intrinsic transition mechanism to detonation of gaseous laminar flames in tubes

Volume 351 (2023), p. 401-427

Published online: 4 December 2023

https://doi.org/10.5802/crmeca.232

Les Comptes Rendus. Mécanique *sont membres du*
Centre Mersenne pour l'édition scientifique ouverte
www.centre-mersenne.org
e-ISSN : 1873-7234

Comptes Rendus
Mécanique
2023, Vol. 351, p. 401-427
https://doi.org/10.5802/crmeca.232

Research article / *Article de recherche*

Intrinsic transition mechanism to detonation of gaseous laminar flames in tubes

Mécanisme intrinsèque de la transition vers la détonation des flammes laminaires en phase gazeuse dans les tubes

Paul Clavin [a]

[a] Aix Marseille Université, CNRS, Centrale Marseille, IRPHE, UMR7342, 49 rue Joliot Curie, BP 146, 13384 Marseille Cedex 13, France
E-mail: paul.clavin@univ-amu.fr

Abstract. The deflagration-to-detonation transition (DDT) on the tip of an elongated flame in a tube is analyzed in the double limit of large activation energy and small Mach number of laminar flames. A spontaneous transition of a self-accelerated laminar flame taking the form of a dynamical saddle-node bifurcation of the flow inside the inner structure of the laminar flame is exhibited by the asymptotic analysis. The predicted critical conditions for the finite-time pressure runaway are in good agreement with the experimental data of the DDT onset in tubes.

Résumé. La transition déflagration–détonation (DDT) sur le bout arrondi d'une flamme allongée (en forme de doigt) dans un tube est analysée dans la double limite d'une grande énergie d'activation et d'un petit nombre de Mach des flammes laminaires. L'analyse asymptotique met en évidence une transition spontanée de la flamme auto-accélérée sous l'effet d'une bifurcation noeud-col de l'écoulement gazeux à l'intérieur de la structure interne de la flamme laminaire. L'analyse prédit des conditions critiques d'emballement en temps fini de la pression qui sont en bon accord avec les données expérimentales de la DDT des flammes laminaires dans les tubes.

Keywords. Deflagration-to-detonation transition, Asymptotic analysis, Finite time singularity, Dynamical saddle-node bifurcation.

Mots-clés. Transition déflagration détonation, Analyse asymptotique, Singularité en temps fini, Bifurcation dynamique noeud-col.

Funding. Agence National de la Recherche (contract ANR-18-CE05-0030).

Manuscript received 29 August 2023, revised and accepted 9 October 2023.

1. Introduction

The deflagration-to-detonation transition (DDT) is a quasi-instantaneous transition (few microseconds) between two opposite regimes of combustion wave. The phenomenon was observed long ago [1]. However, after more than a century of experimental works and decades of numerical

studies reported in an extensive literature, DDT is not yet understood [2,3]. Gaseous detonations are supersonic combustion waves involving a pressure rise $\Delta p/p$ ranging from 20 to 50 and propagating with a velocity $\mathscr{D}$ between 2000 m/s and 3500 m/s under normal conditions. By contrast, laminar flames are quasi-isobaric reaction–diffusion waves characterized by a markedly subsonic velocity and a negligible pressure drop $\Delta p/p \ll 1$. No other quasi-steady combustion waves exist between these two extreme propagation regimes. The abrupt transition is explained here by a finite time singularity of the one-dimensional reacting flow associated with a self-accelerated flame produced by an extension increase in elongation of the multidimensional flame front.

Coupling reaction–diffusion waves with compressible flows is a challenging problem that has been recently solved analytically by an asymptotic analysis [4]. For the sake of self-consistency, this analysis is reproduced in Sections 3–5 with additional comments in Section 3 on the compatibility of the basic assumptions of the asymptotic analysis and the conditions of the DDT experiments. Moreover, an original stability analysis is presented in Section 6. The Sections 3–5 are technical and non easy to follow by non specialists of flame theory. However the conditions of the analysis discussed in Section 3 and their relevance for the experiments can be easily understood as follows. The asymptotic analysis is based on two limits: a large thermal sensitivity of the reaction rate $\beta \gg 1$ and a small Mach number of laminar flames $\varepsilon \ll 1$. The first limit leads to concentrate the chemical heat release in a reaction sheet at high temperature while the second one leads to a multiple scale flow; the length scale of the compressible flows outside the quasi-isobaric flame structure is much larger than the flame thickness by a factor $1/\varepsilon$, so that, to leading order, the pressure is quasi-uniform across the flame thickness and its compression-induced time variation is mall of order ε. The key points of the asymptotic analysis are a distinguished limit $\varepsilon\beta$ of order unity $\varepsilon\beta = O(1)$ and an elongation rate smaller than the inverse of the transit time across the flame, $\epsilon \ll 1$. The condition $\varepsilon\beta = O(1)$ allows to study the whole compression-induced dynamics for small variations of the flame temperature, of order $1/\beta$. For a small elongation rate, assuming the ordering $\varepsilon \ll \epsilon \ll 1$, the compression-induced unsteadiness is described by a perturbation analysis keeping the pressure uniform in the flame structure. Moreover assuming a flame thickness d smaller than the tube radius r, $d/r \ll 1$ of order ε, $d/r = O(\varepsilon)$, the flame front around the point at which the DDT onset occurs is quasi-planar because the pressure propagates in the transverse direction faster than the longitudinal dynamics.

After reading the background in Section 2 and a quick look to the formulation of the problem in Sections 3.1 and 3.2, the physics-oriented readers can skip Sections 4–6 to go directly to Section 7 where the nonlinear dynamics is discussed. There, a dynamical saddle-node bifurcation of the reacting flow is identified, exhibiting an intrinsic one-dimensional mechanism of DDT.

2. Background

The basic properties of combustion waves are well known for a long time [3]. They are briefly recalled below with a particular attention paid to the order of magnitude of the physical mechanisms involved in the DDT. The existing experimental results and the previous analyses that are relevant for the present analysis are also recalled at the end of this section.

2.1. *Planar laminar flames*

In gas, the laminar flame velocity relative to the unburned gas U_L ranges from 10 cm/s in weakly energetic gaseous mixture to 10 m/s in the most energetic ones. The flame temperature T_b is in the range 1800–3100 K and the reaction rate in a flame is typically $1/\tau_r \approx 10^6$ s^{-1}. The chemical kinetic network of gaseous combustion is complex explaining why combustion cannot proceed below a crossover temperature $T_c \in$ [850–1200 K] [5]. However, at high temperature

$T > 1500$ K the flame dynamics can be described with a good accuracy by a reaction rate governed by inelastic binary collisions of molecules of reactant whose collision energy is larger than an activation energy $\mathscr{E}$ much larger than the thermal agitation $k_B T$. Typically, the reduced activation energy[1] $\beta \equiv \mathscr{E}/k_B T_b > 1$ is between 2 in energetic mixtures (stoichiometric H_2/O_2 or C_2H_2/O_2 mixtures in which the flame temperature is large $T_b > 3000$ K) and 8 in hydrocarbon–air flames ($T_b \approx 2000$ K). According to the kinetic theory of gas, the reaction rate $1/\tau_r$ at high temperature is expressed in terms of the collision frequency $1/\tau_{\rm coll}$ in the form of an Arrhenius law $\tau_{\rm coll}/\tau_r \propto \beta e^{-\beta}$. The Zeldovich–Frank-Kamenetstskii (ZFK) analysis [7] in the limit $\beta \gg 1$ shows that the laminar flame velocity relative to the burned gas U_b is expressed in terms of the molecular diffusivity $D \approx a^2 \tau_{\rm coll}$ (a is the sound speed) and the reaction rate in the form $U_b \propto \beta^{-3/2}\sqrt{D_b/\tau_{rb}} \approx a_b e^{-\beta/2}/\beta$ where the subscript b refers to the burned gas, see [3] for a didactic presentation. The flame thickness d and the transit time t_b of a fluid particle across the flame are respectively $d = D_b/U_b \approx 2{-}4\times 10^{-1}$ mm and $t_b = d/U_b \propto \beta^3 \tau_{rb} \approx 10^{-4}$ s under normal conditions. Due to a large activation energy, the flame Mach number $\varepsilon \equiv U_b/a_b \propto e^{-\beta/2}/\beta$ is small, about 10^{-3} in hydrocarbon–air mixtures and $10^{-2} - 10^{-1}$ in the most energetic mixtures. In any cases, the pressure drop across the flame is negligible $\Delta p/p \approx \varepsilon^2$. Planar flames are unstable against transverse disturbances (Darrieus–Landau instability), however, as shown by Zeldovich, the instability does not concern the tip of a curved flames in tubes, see [3] for a review.

2.2. *Gaseous detonations*

Detonations consist of a strong inert shock of few mean free paths thick ($\approx a\tau_{\rm coll}$) followed by a macroscopic zone of reaction. The flow of compressed gas is subsonic relatively to the shock but not smaller than $a_N/10$, the subscript N denoting the state of compressed gas adjacent to the shock (Neumann state). The diffusive transports are negligible across the reaction zone (thickness $\approx a_N \tau_{rN}/10$) because the ratio $\tau_{rN}/\tau_{\rm coll}$ is a large number, typically $\tau_{rN}/\tau_{\rm coll} > 10^3$. A condition for the existence of a detonation is that the inert shock is strong enough for making the Neumann gas temperature T_N larger than the crossover temperature, $T_N > T_c$ so that the detonation Mach number is always substantially larger than unity $M \equiv \mathscr{D}/a_o > 4.5$, a_o denoting the sound speed ahead of the shock. Moreover, independently from chemical kinetic considerations, the conservation of mass, momentum and energy implies that the Mach number of a planar detonation in steady state cannot be smaller than a lower bound called Chapman–Jouguet (CJ) $M_{CJ} \approx 5$. The marginal CJ detonation is a self-propagating regime characterized by a sonic condition in the burned gas. All the other regimes $M > M_{CJ}$, called overdriven detonations, are piston-supported with a subsonic burned gas flow (relatively to the lead shock).

2.3. *Experimental data. Unexplained results*

Several DDT experiments have been performed in long smooth-walled tubes filled with stoichiometric H_2/O_2 or C_2H_4/O_2 mixtures. We limit the attention to those performed under the conditions considered in the present analysis. The reactive mixture is ignited on a closed end of the tube which is long enough for the DDT onset to occur before reflected shocks interact with the flame. In micro-scale tubes (radius $\approx$ few mms) the front of the laminar flame just before transition is elongated and the flow is laminar [8] see Figure 1. The DDT is also observed after the middle of the channel in an open-ended tubes [9], this case is not considered here, even though the DDT mechanism is not so different. The DDT is more difficult to analyze in larger tubes because the wrinkled flame front can become turbulent [10], the problem becoming stochastic in

[1] In real combustible mixtures governed by a complex chemical network of elementary reactions, the activation energy is replaced by the thermal sensitivity of the exothermic reaction rate [6].

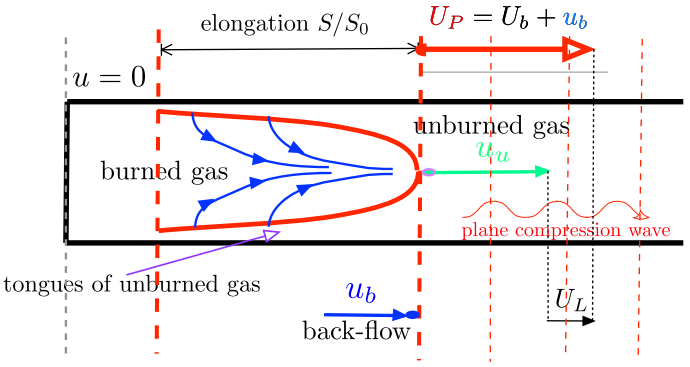

Figure 1. Sketch of an elongated flame in a smooth-walled tube.

nature. Conclusions can nevertheless be drawn since the salient features of the abrupt transition in moderately large tubes are not so different, especially as the flow stays laminar ahead of the wrinkled flame front [11, 12]. Salient features of DDT were pointed out in the sixties by the pioneering experiments of Oppenheim and co-workers [10]: the spontaneous detonation onset is a local phenomenon concerning small explosion centers. In some turbulent flames the explosion center is located in the boundary layer [10]. In such cases, the DDT is more likely associated with the Zeldovich gradient mechanism [13] reinforced by compressible effects [3]. This case is not considered here. The attention is focused on the transition of laminar flames accelerated by a self-generated convection flow as in the 2010 experiments and numerical simulations [11, 12] in which the flow of unburned gas is laminar and the explosion center is located on the flame front outside the boundary layer. The flow considered in the analysis is sketched in Figure 1.

In tubes of moderate transverse size (few cm in diameter) the non-dimensional surface area (reduced by the cross section surface of the tube) $\Sigma(t) > 1$ of a elongated flame first increases exponentially up to the transient formation of a tulip-shaped flame [14]. Then, the finger shaped front is restored quickly and $\Sigma(t)$ increases again but more slowly up to an abrupt detonation onset [11,12]. In micro-scale tubes there is no transitory formation of tulip flame; the finger flame keeps an elongated form with a growing length before an eventual DDT onset [8]. Considering a quasi-steady flow of burned gas sketched in Figure 1 and assuming a laminar flame speed U_b approximately constant all over the flame surface, the mass conservation leads to a speed of the tip in the laboratory frame in a form extensively used in turbulent flame theory

$$U_P \approx \Sigma U_b. \tag{1}$$

The increase in surface-area $\Sigma > 1$ produces a longitudinal flow of burned gas with which the leading edge of the flame front is convected at the velocity U_P in (1), see Figure 1. Acceleration of the convection flow by the rate of surface-area increase ($\mathrm{d}\Sigma/\mathrm{d}t > 0$) accelerates the flame on the tip. Generally speaking, the detonation onset occurs spontaneously when appropriate local conditions are attained in the unburned gas adjacent to the leading edge of the self-accelerating flame [2]. This occurs in the experiments [11, 12] when the overall speed of the flame on the tip reaches a critical value $U_P^* = \Sigma^* U_b^*$ which is comparable to the local sound speed a_b^* [9, 11, 12]. The critical elongation Σ^* is typically in the range 5–10. Therefore, according to the experimental data showing that U_P^* is close to a_b^*, a large laminar flame velocity is involved at the critical condition $U_b^* \approx a_b^*/\Sigma^*$. Such a large U_b can be obtained by the small compressional heating of downstream-running compression waves as long as the thermal sensitivity of the laminar flame

is large enough.[2] However, as a rule of thumb, the temperature of the compressed unburned gas stays well below the crossover temperature T_c so that the mixture just ahead of the flame remains chemically frozen.

Therefore, DDT can be explained neither by the Zeldovich gradient mechanism [13] (since self-ignition cannot occur) nor by a pressure pulse of downstream running compression waves in phase with the rate of heat release. The latter mechanism would require a sonic condition $U_b = a_b$ which can never be fulfilled in laminar flames,[3] no matter how large the surface area of the elongated front Σ and the tip velocity U_P. The objective of the present analysis is to explain the detonation onset in the 2010 experiments and numerics [11, 12] of laminar flames in tubes.

2.4. *Previous analyses*

The previous one-dimensional analyses that are useful for the analysis presented in this article are summarized below.

2.4.1. *First analyses (1989)–(2014): Self similar solutions and 1-D numerical simulations*

A key mechanism underlying the DDT was identified in 1989 by a pioneering analysis [15] which was overlooked during 25 years. Treating a wrinkled flame as a planar discontinuity propagating in a tube from a closed end at a velocity U_P equal to the laminar flame velocity multiplied by a wrinkling factor $s > 1$, s being equivalent to Σ in (1), $U_P = sU_b$, Deshaies and Joulin [15] considered the self-similar solutions constituted by a lead shock followed by the wrinkled flame. In such solutions the two planar discontinuities (flames and lead shock) propagate at constant velocity (subsonic relatively to the gas for the flame and supersonic for the shock). Deshaies and Joulin showed that the self-similar solutions no longer exist above a critical value of the wrinkling factor s^* close 10 in ordinary condition. This is due to a nonlinear thermal feed back loop between the flame and the lead shock: the laminar flame velocity U_b increases strongly with the gas temperature which increases with the strength of the shock, the later increasing in turn with U_b through the flow induced upstream of the flame by the density jump across the flame. The critical turning point $s = s^* \approx 10$ corresponds to a gas temperature well below T_c. Nevertheless, unsteady numerical solutions of planar flames show a runaway of the solution few time after a quasi-isobaric ignition on the closed end of a tube provided the reaction rate is artificially increased by a factor equal to (or larger than) $s^{*2} \approx 10^2$ [16] so that the laminar flame velocity is ten times larger than the usual one obtained with an Arrhenius law and the molecular diffusive transport that are controlled by the kinetic theory of gas. Even though the flame model is not satisfactory from a physical point of view, these numerical solutions are instructive since they illustrate an intrinsic DDT mechanism of a subsonic combustion waves.

2.4.2. *Quasi-steady one-dimensional back-flow model. Recent analytical studies 2021–2023*

Motivated by the works [15, 16], a one-dimensional model [6] was recently developed and studied analytically to elucidate an intrinsic DDT mechanism of planar flame sustained by a reaction rate compatible with the kinetic theory of gas. The key mechanism is the longitudinal convective motion of the flame by the self-induced flow of burned gas, called back-flow in [6, 17, 18]. The latter results from the combustion of the lateral part of the flame front quasi-parallel to the tube wall, see Figure 1. The tip of the finger-shaped flame is considered as a planar

[2] In very energetic mixtures the thermal sensitivity includes the temperature power laws in the pre-factor of the Arrhenius factor in the expression of the laminar flame velocity [6].

[3] The sonic condition defining the so-called *CJ deflagration* is sometimes referred to as a possible DDT mechanism of turbulent flames [2]. The author of the present article does not share this point of view since a turbulent flame brush is constituted by elements of laminar flames that are accelerated by a self-generated convection flow.

flame perpendicular to the axial flow of burned gas impinging the flame from behind with the velocity u_b. The resulting speed of the flame in the laboratory frame is $U_P = u_b + U_b$, the subscript P being for piston since the flame acts as a semi-transparent piston. Following [14] when the gas behind the foot of the finger flame is at rest as in Figure 1 (closed end), the back-flow u_b is proportional to the surface area $\mathscr{S}$ of the lateral part of the flame front. Considering the elongated flame as quasi-cylindrical and introducing the elongation parameter $S = \mathscr{S}/\mathscr{S}_0$ where $\mathscr{S}_0$ is the cross section area of the tube, one gets, using the same approximations as in (1), $u_b \approx SU_b$, $S > 0$, leading to $U_P = u_b + U_b \approx \Sigma U_b$ with

$$\Sigma = S + 1 \geqslant 1, \quad U_P = \Sigma U_b, \quad u_b \approx SU_b. \tag{2}$$

The key point is that the speed of the flame front U_P (and thus the flow u_b) is proportional to the laminar flame velocity U_b. This is responsible for a thermal feed-back loop similar to that described long ago [15], leading to the same phenomenology discussed now. If the inner structure of the laminar flame is in steady state, the flow of unburned and burned gas adjacent to the flame, respectively u_u and u_b, are $u_u = U_P - U_L$ and $u_b = U_P - U_b$ where U_L and U_b are the laminar flame velocity relative to the unburned and burned gas respectively. According to the isobaric condition and the mass conservation, the ratio $U_b/U_L = 1/(1-q)$ is given by the reduced heat release $q \equiv Q/(c_p T_b) < 1$ that controls the increase of flow velocity across the flame $u_u - u_b = U_b - U_L = qU_b$. Considering the flame as a semi-transparent piston ($u_u < U_P$), it was shown [6] that, as in the pioneering analysis [15], the self-similar solutions $U_P(\Sigma)$ have a turning point namely a maximum of the curve $\Sigma(U_P)$ for a critical elongation $\Sigma = \Sigma^*$ above which there is no more self similar solution and below which there are two branches of self-similar solutions $\Sigma < \Sigma^*$: $U_P^-(\Sigma) < U_P^+(\Sigma)$, $U_P^+(\Sigma^*) = U_P^-(\Sigma^*) \equiv U_P^*$ such that $\mathrm{d}\Sigma/\mathrm{d}U_P^- > 0$ (physical branch), $\mathrm{d}\Sigma/\mathrm{d}U_P^+ < 0$ and $\mathrm{d}\Sigma/\mathrm{d}U_P^\pm|_{U_P^*} = 0$. It was also shown [6] that the turning point (Σ^*, U_P^*) corresponds with a relatively good accuracy to the DDT onset in the 2010 experiments [11, 12].

The basic assumption of self-similar solutions, namely a uniform flow of unburned gas between the flame and the lead shock, is a major weakness of such solutions. The unsteady and non uniform compression waves $u_{\mathrm{ext}+}(\mathrm{x}, t)$ that are generated in the unburned gas by the accelerating flame have been considered for a long time as an essential ingredient of the gaseous DDT in tubes [2]. Still treating the flame as a semi-transparent piston, the problem was extended recently to take into account the unsteady compression waves in the unburned gas ahead of the flame [17, 18]. The so-obtained solutions have the same structural form as the self-similar solutions: there is two branches of solutions $U_P^\pm(\Sigma)$ merging at a turning point (Σ^*, U_P^*). However, the latter is now depending on the initial condition and presents an upper bound. Starting from a self-similar solution and assuming that the solution follows the physical branch of the self-similar solutions $U_P^-(\Sigma)$ when the elongation increases slowly $\Sigma(t)$, $(1/\Sigma)\mathrm{d}\Sigma/\mathrm{d}t \ll 1/t_b$, the flame acceleration diverges at the turning point $\mathrm{d}U_P^-/\mathrm{d}\Sigma|_{\Sigma=\Sigma^*} = \infty$. This structural property of the turning point $\Sigma = \Sigma^*$ ($p = p^*$, $T_b = T_b^*$, $U_b = U_b^*$) implies that the gradient of the unsteady flow of unburned gas diverges on the flame front when the critical elongation is reached [6, 17, 18]. Even though no runaway of pressure and temperature is described for an accelerating flame considered as a semi-transparent piston, the finite time singularity of the flow suggests the shock formation inside the flame structure that could explain the detonation onset.

The flame dynamics in [17, 18] is based on two assumptions: firstly, both burned gas flow and inner flame structure are assumed in steady state and secondly, these quasi-steady solutions are assumed stable. Here, the stability limits of the quasi-steady solutions are analyzed. Moreover, removing the quasi-steady assumptions, the non linear dynamics is studied in the stable domain for an elongation increasing with the time. By contrast with the previous results, a finite-time runaway of the pressure responsible for the detonation onset is exhibited.

3. Formulation

We consider a quasi-planar geometry on the tip of the elongated flame sketched in Figure 1 and an axial back-flow u_b on the hot side of the flame as before. We will not discuss the origin of the increase in surface area $\Sigma(t)$ responsible for the acceleration of the tip $\mathrm{d}U_p/\mathrm{d}t > 0$. The elongation of a laminar flame in a tube with stick walls is due to the stretching of the flame front which is anchored inside the boundary layer on the tube wall while the flow in the bulk is large. The elongation is governed by the quasi-isobaric expansion of the gas across the flame front while the abrupt DDT is a consequence of a quite different mechanism, namely the compression waves in the external flows. In the following, the attention is focused on the second mechanism and the dynamics is analyzed for a small growth rate of elongation considered as a given parameter. The initial condition (labelled i) is constituted by a self-similar solution whose lead shock is at infinity; the initial back flow u_{bi}, laminar flame speed U_{bi}, flame temperature T_{bi} and flame speed in the laboratory frame $U_{Pi} = u_{bi} + U_{bi}$ are constant before the elongation starts to increase, $t \leqslant 0$ and the flow of unburned gas ahead of the flame $u_{\mathrm{ext}+}$ is initially constant and uniform

$$t = 0: \quad u_b = u_{bi}, \quad U_b = U_{bi}, \quad U_P = U_{Pi}, \quad u_{\mathrm{ext}+} = u_{ui} \tag{3}$$

with, according to the mass conservation across a steady isobaric flame,

$$u_{ui} \equiv u_{bi} + qU_{bi} < U_{Pi}, \quad 0 < U_{Pi} - u_{ui} = (1-q)U_{bi} < U_{bi} \quad \text{where } q \equiv Q/c_p T_{bi} < 1. \tag{4}$$

Denoting the initial elongation $S_i > 0$, we consider a time dependent elongation in the form

$$S(t) = [1 + \epsilon t/t_b]S_i, \tag{5}$$

the new parameter ϵ (not to be confused with $\varepsilon \equiv U_b/a_b \ll 1$) characterizing the growth rate of elongation relative to the inverse of the transit time across the planar flame t_b.

3.1. *Distinguished limits*

The analysis of the flow sketched in Figure 1 is performed in the limit of small flame Mach number $\varepsilon \equiv U_b/a_b \ll 1$ using the ZFK flame model [7] in the limit $\beta \gg 1$ for which the thickness of the reaction zone d/β shrinks to zero. The same distinguished limit of large thermal sensitivity $\beta \gg 1$ and small Mach number of the laminar flame $\varepsilon \ll 1$ as in the previous analyses [15, 18] is used here in the asymptotic study of the dynamics associated with (5)

$$\varepsilon \to 0, \quad \beta \to \infty: \quad (\gamma - 1)\beta\varepsilon S_i = O(1), \quad S^*/S_i > 1, \quad S^*/S_i = O(1). \tag{6}$$

The critical elongation of the quasi-steady solutions, obtained using the ZFK expression $\varepsilon \equiv U_b/a_b \approx \mathrm{e}^{-\beta/2}/\beta$, is not larger than 0.05. A key point in the range of parameters (6) is that small variations of acoustic pressure (of order ε) induce variations of back flow u_b and laminar flame speed U_b of order unity. The analysis takes advantage of two simplifications: firstly, a negligible pressure drop across the flame $\Delta p/p \approx \varepsilon^2$ and secondly a scale separation of the flow discussed lengthly in Section 3.5.2. The acceleration-induced variation of pressure is of order ε so that the ε-terms are retained in the perturbation analysis while the ε^2-terms are neglected.

3.2. *Validity of the one-dimensional approximation*

The one-dimensional model is relevant under conditions that are discussed now. For a curvature radius of the tip of the same order of magnitude as the tube radius r, the transverse fluxes inside the flame structure are negligible in front of the compressional heating when the condition $D/r^2 \approx U_b d/r^2 \ll \varepsilon/t_b \approx \varepsilon U_b/d$ is fulfilled so that the curvature effects on the flame are negligible in the perturbation analysis retaining ε-terms. This leads to the condition $(d/r)^2 \ll \varepsilon$.

Another condition is required for making the the compression waves quasi-planar and propagating in the longitudinal direction; the time to make the pressure homogeneous in the transverse direction should be smaller than the characteristic time of evolution. Using (5) $\mathrm{d}S/\mathrm{d}t = \epsilon S_i/t_b$, this condition can be written $\epsilon S_i/S \ll (a/r)t_b = (a/U_b)(d/r) = (1/\varepsilon)d/r$ yielding $\epsilon \ll (1/\varepsilon)d/r$ for $S^*/S_i = O(1)$. Combined together the two conditions provide the range of tube radius $\varepsilon\epsilon \ll d/r \ll \sqrt{\varepsilon}$ requiring the ordering $\epsilon \ll 1/\sqrt{\varepsilon}$. Being proportional to the time derivative of the pressure in the energy equation, see (18) below, the parameter measuring the compressibility effect on the inner flame structure is $\varepsilon\epsilon$ which is larger than the neglected ε^2-terms if $\varepsilon \ll \epsilon$. Therefore, the non-dimensional elongation rate ϵ and the tube radius r/d should be related to the Mach number of the laminar flame velocity ε by the following ordering

$$\varepsilon \ll \epsilon \ll 1/\sqrt{\varepsilon}, \quad \varepsilon\epsilon \ll d/r \ll \sqrt{\varepsilon} \Leftrightarrow \frac{1}{\sqrt{\varepsilon}} \ll \frac{r}{d} \ll \frac{1}{\varepsilon\epsilon}. \tag{7}$$

The second conditions in (7) is automatically satisfied if $\varepsilon r/d$ is of order unity and $\epsilon \ll 1$. Therefore the quasi-planar approximation on the tip is valid for $r/d = O(1/\varepsilon)$ and $\epsilon \ll 1$ under a more restrictive condition than in (7) for the non-dimensional growth rate ϵ,

$$\varepsilon \ll \epsilon \ll 1, \quad \varepsilon(r/d) = O(1), \tag{8}$$

in good agreement with the range of parameters characterizing the low pressure flames before the DDT onset in the 2010 experiments [11,12] , $\varepsilon \approx 10^{-2}$, $\epsilon \approx 10^{-1}$, $r/d \approx 50$.

To summarize a one-dimensional analysis performed in the distinguished limit (6) of large activation energy and small Mach number of laminar flames is relevant under the condition (8).

3.3. *Non-dimensional constitutive equations*

Choosing the burned gas of the initial flame as reference state and denoting T_{ui} the temperature of the unburned gas, ρ_{bi} the density of the burned gas in the initial state, the reference temperature, velocity, density and pressure are

$$T_{bi} \equiv T_{ui} + Q/c_p, \quad U_{bi} \equiv U_b(T_{bi}), \quad \rho_{bi}, \quad p_{bi} = (c_p - c_v)\rho_{bi}T_{bi}. \tag{9}$$

Using for unit length and time the initial flame thickness and transit time $d = D_{bi}/U_{bi}$ and $t_{bi} = d_{bi}/U_{bi} = D_{bi}/U_{bi}^2$ where D_{bi} is the molecular diffusion coefficient in the burned gas, the non-dimensional variables are

$$\tau \equiv t/t_{bi}, \quad \xi \equiv (\mathrm{x} - X_P)/d_{bi}, \tag{10}$$

$$r \equiv \rho/\rho_{bi}, \quad \mathrm{v} \equiv u/U_{bi}, \quad \pi \equiv p/p_{bi}, \quad \theta \equiv T/T_{bi}, \quad \mathrm{v}_P \equiv U_P/U_{bi}, \tag{11}$$

where $\mathrm{x} = X_P(t)$ is the instantaneous position of the reaction sheet of the ZFK flame ($\xi = 0$), $u(\mathrm{x},t)$ is the flow velocity and $U_P(t) \equiv \mathrm{d}X_P/\mathrm{d}t$ the propagation velocity of the flame, both velocities being relative to the laboratory frame. A perfect gas law is assumed in the following $r = \pi/\theta$.

As for the study of vibratory flames [19], the analysis of the unsteady flame structure is performed with the mass-weighted coordinate z, using the change of variables $(\xi,\tau) \to (z,\tau)$

$$z \equiv \int_0^\xi r(\xi',\tau)\mathrm{d}\xi', \quad \frac{\partial}{\partial\xi} = r\frac{\partial}{\partial z} = \frac{\pi}{\theta}\frac{\partial}{\partial z}, \quad \left.\frac{\partial}{\partial\tau}\right|_\xi + (\mathrm{v} - \mathrm{v}_P(\tau))\frac{\partial}{\partial\xi} = \left.\frac{\partial}{\partial\tau}\right|_z - m(\tau)\frac{\partial}{\partial z} \tag{12}$$

where $m(\tau)$ is the instantaneous reduced mass flux across the reaction zone

$$m(\tau) = r(0,\tau)[\mathrm{v}_P(\tau) - \mathrm{v}(0,\tau)] = \frac{\pi(0,\tau)}{\theta(0,\tau)}[\mathrm{v}_P(\tau) - \mathrm{v}(0,\tau)] > 0. \tag{13}$$

Introducing the Mach number of the laminar flame, the reduced heat release and the reduced activation energy

$$\varepsilon \equiv \frac{U_{bi}}{a_{bi}} \approx 10^{-2}, \quad q \equiv \frac{Q}{c_p T_{bi}} \approx 0.7, \quad \beta \equiv \frac{\mathscr{E}}{k_B T_{bi}} = 4 - 8, \tag{14}$$

and assuming unity Lewis and Schmidt numbers with a diffusion coefficient verifying $\rho^2 D =$ constant for simplicity, the constitutive equations in a planar geometry for reactive flows governed by a one-step chemical reaction are [19]

$$\text{continuity } \frac{\partial \mathrm{v}}{\partial z} = \left[\frac{\partial}{\partial \tau} - m(\tau)\frac{\partial}{\partial z}\right]\frac{\theta}{\pi},$$
$$= \frac{1}{\pi}\left[\frac{\partial}{\partial \tau} - m(\tau)\frac{\partial}{\partial z}\right]\theta - \frac{\theta}{\pi^2}\left[\frac{\partial}{\partial \tau} - m(\tau)\frac{\partial}{\partial z}\right]\pi \tag{15}$$

$$\text{momentum } \left[\frac{\partial \mathrm{v}}{\partial \tau} - m(\tau)\frac{\partial \mathrm{v}}{\partial z} - \frac{\partial^2 \mathrm{v}}{\partial z^2}\right] = -\frac{1}{\gamma\varepsilon^2}\frac{\partial \pi}{\partial z} \tag{16}$$

$$\text{species } \left[\frac{\partial Y}{\partial \tau} - m(\tau)\frac{\partial Y}{\partial z} - \frac{\partial^2 Y}{\partial z^2}\right] = w(\theta, Y), \quad Y(z,\tau) \in [0,1] \tag{17}$$

$$\text{energy } \left[\frac{\partial \theta}{\partial \tau} - m(\tau)\frac{\partial \theta}{\partial z} - \frac{\partial^2 \theta}{\partial z^2}\right] = q\,w(\theta, Y) + \frac{(\gamma-1)}{\gamma}\frac{\theta}{\pi}\left[\frac{\partial \pi}{\partial \tau} - m(\tau)\frac{\partial \pi}{\partial z}\right] + (\gamma-1)\varepsilon^2\left(\frac{\partial \mathrm{v}}{\partial z}\right)^2 \tag{18}$$

where $1-Y$ is the reduced mass fraction of reactant ($Y=0$ in the initial mixture) and $w(\theta, Y)$ is the non-dimensional reaction rate. For a one-step reaction of order 2 governed by an Arrhenius law with a large activation energy one has

$$w(\theta, Y) = \frac{(q\beta)^3}{8}\frac{\pi_b}{\theta_b}(1-Y)^2 \mathrm{e}^{\beta(\theta-1)}. \tag{19}$$

The perfect gas law $r = \pi/\theta$ has been used in (15) and (18) to eliminate the density. The main interest of the mass-weighted coordinates is the simpler form of the Lagrangian derivative $\partial/\partial\tau + m(\tau)\partial/\partial z$ instead of $r(\xi,\tau)[\partial/\partial\tau + \mathrm{v}(\xi,\tau)\partial/\partial\xi$. When the dissipative terms (heat conduction, viscosity and reaction rate) are neglected, (18) takes the form of the entropy wave in an inert gas subjected to adiabatic compression $\delta\theta/\theta = [(\gamma-1)/\gamma]\delta\pi/\pi$

$$\frac{1}{\theta}\left[\frac{\partial \theta}{\partial \tau} - m(\tau)\frac{\partial \theta}{\partial z}\right] - \frac{(\gamma-1)}{\gamma}\frac{1}{\pi}\left[\frac{\partial \pi}{\partial \tau} - m(\tau)\frac{\partial \pi}{\partial z}\right] = 0. \tag{20}$$

3.4. *Limit of large activation energy $\beta \gg 1$. Boundary conditions on the reaction sheet*

The ZFK analysis [7] has been extended more than forty five years ago to the unsteady flame structure [20]. In the limit of large activation energy, small temperature disturbances of order $1/\beta$ have a large effect and the reaction is localized at $z=0$ in a reaction sheet of thickness $1/\beta$ smaller than the flame thickness. Jump conditions are obtained by integrating the balance between diffusion and reaction rates across the thin reaction zone

$$z \leqslant 0: \quad Y = 1,$$
$$z = 0: \quad Y = 1, \quad \theta = \theta_b(\tau), \quad (\theta_b - 1) = O(1/\beta), \quad \mathrm{v} = \mathrm{v}_b(\tau) \equiv \frac{u_b(\tau)}{U_{bi}} \tag{21}$$

$$\beta \gg 1, \quad \beta(\theta_b - 1) = O(1): \quad \left.\frac{\partial \theta}{\partial z}\right|_{z=0^+} = -q \exp\left[\frac{\beta}{2}(\theta_b - 1)\right] + O(1/\beta) \tag{22}$$

$$\left.\frac{\partial \theta}{\partial z}\right|_{z=0^-} = \left.\frac{\partial \theta}{\partial z}\right|_{z=0^+} - q\left.\frac{\partial Y}{\partial z}\right|_{z=0^+} + O(1/\beta^2), \tag{23}$$

$z = 0^+$ and $z = 0^-$ denoting respectively the preheated zone side of the reaction zone and the exit on the burned-gas side. Equation (22) is a chemical-kinetics relation valid to order unity expressing the balance between the heat flux entering the preheated zone and the rate of chemical energy released in the reaction zone. Equation (23) is an isobaric conservation of total energy (thermal plus chemical), valid up to first order $1/\beta$ (included). The flow velocity u does not vary across the reaction zone in the limit $\beta \ll 1$ and is equal to the back-flow $u = u_b$. By definition, the instantaneous laminar flame velocity is $U_b(\tau) \equiv U_P(\tau) - u_b(\tau)$ where U_P is the velocity of the

reaction sheet in the laboratory frame. Introducing the non-dimensional back-flow, velocity of the reactive sheet and laminar flame velocity

$$\mathrm{v}_b(\tau) \equiv u_b(\tau)/U_{bi}, \quad \mathrm{v}_P(\tau) \equiv U_P(\tau)/U_{bi}, \quad \mathrm{u}_b(\tau) \equiv U_b(\tau)/U_{bi}, \tag{24}$$

one has, by definition,

$$\mathrm{u}_b(\tau) = \mathrm{v}_P(\tau) - \mathrm{v}_b(\tau), \quad \mathrm{v}_{bi} = \mathrm{v}_{Pi} - 1 \tag{25}$$

where the subscript i denotes the initial condition $\tau = 0 : \mathrm{u}_b = \mathrm{u}_{bi} = 1$, $\mathrm{v}_P = \mathrm{v}_{Pi}$, $\mathrm{v}_b = \mathrm{v}_{bi}$, $\theta_b = \theta_{bi} = 1$. According to the conservation of mass and energy across a quasi-isobaric flame, the initial non-dimensional temperature and flow velocity of the unburned gas far ahead of the flame are respectively $1 - q$ and $\mathrm{v}_{bi} + q$.

To leading order in the distinguished limit (6) for $\beta \gg 1$ and $\varepsilon \ll 1$, $(\theta_b - 1) = O(1/\beta)$ and $\pi_b - 1 = O(\varepsilon)$, the non-dimensional mass flux (13) and laminar flame velocity (25) are equal

$$\beta \gg 1, \quad \varepsilon \ll 1 : \quad m(\tau) \approx \mathrm{u}_b(\tau). \tag{26}$$

3.5. *Limit of small flame Mach number $\varepsilon \ll 1$*

The coupling of reaction–diffusion mechanisms and compressible effects in an accelerating flame gets simpler in the limit of small Mach number of the laminar flame velocity.

3.5.1. *Two length-scales problem*

As soon as the flame accelerates ($\mathrm{d}\mathrm{v}_P/\mathrm{d}\tau > 0$) downstream-running compression waves are sent in the unburned gas outside the flame structure ($z \gg 1$). They are denoted by the subscript $ext+$ (short notation for upstream external flow). The problem being hyperbolic, the downstream boundary conditions far ahead of the flame corresponds to the initial solution,

$$\begin{aligned} z \to \infty: \quad & \pi \approx 1 + O(\varepsilon^2), \quad Y = 0, \quad \theta_{\mathrm{ext}+} \to 1 - q + O(\varepsilon^2), \\ & \mathrm{v}_{\mathrm{ext}+} \to (\mathrm{v}_{\mathrm{ext}+})_i = \mathrm{v}_{bi} + q. \end{aligned} \tag{27}$$

The neglected terms are of the same order of magnitude as the pressure jump across a laminar flame $\Delta p/p = O(\varepsilon^2)$ given by the steady-state version of (16). According to the previous result [18], the initial condition can be chosen not too far from the critical condition so that the modification of the flow ahead of the flame is not larger than the laminar flame velocity $\delta u_{\mathrm{ext}+} = O(U_b)$, $\delta \mathrm{v}_{\mathrm{ext}+} \equiv \mathrm{v}_{\mathrm{ext}+} - (\mathrm{v}_{\mathrm{ext}+})_i = O(1)$. Anticipating the same order of magnitude of pressure variation as in acoustics (to be checked a posteriori) one gets $\delta p = O(\rho a U_b)$, $\delta\pi \equiv 1 - \pi = O(\epsilon)$

$$\varepsilon \ll 1: \quad \pi = 1 + \varepsilon\,\pi_1, \quad \theta_{\mathrm{ext}+} = 1 - q + \varepsilon\,(\theta_{\mathrm{ext}+})_1, \quad \pi_1 = O(1), \quad (\theta_{\mathrm{ext}+})_1 = O(1). \tag{28}$$

Therefore, the new shocks generated by the flame acceleration are weak (intensity of order ε) with an entropy jump is of order ε^3 [3]. Limiting the attention to the first order in the limit of small Mach number, the jump across the acceleration-induced shocks are negligible. Moreover, heat conduction and viscosity involving terms of order ε^2, the entropy production is also negligible upstream from the flame. The flame running from left to right faster than the flow of unburned gases $\mathrm{v}_P > \mathrm{v}_{\mathrm{ext}+}$, $m(\tau) > 0$, the entropy wave (20) propagates from right to left in the reference frame attached to the flame so that there is no downstream running entropy flux coming from the flow ahead of the flame. Therefore the acceleration-induced flow in the unburned gas is quasi-isentropic to first order in the limit $\varepsilon \ll 1$. This external flow of unburned gas is a downstream-running acoustic wave, namely a solution to the non-dissipative version of (15)–(18), see below (38),

$$\varepsilon \ll 1: \quad \frac{\partial \mathrm{v}_{\mathrm{ext}+}}{\partial z} \approx -\frac{(1-q)}{\gamma}\varepsilon\frac{\partial \pi_1}{\partial \tau}, \quad \frac{\partial \mathrm{v}_{\mathrm{ext}+}}{\partial \tau} \approx -\frac{\varepsilon}{\gamma}\frac{\partial \pi_1}{\partial z_1} \Rightarrow \frac{\partial^2 \pi_1}{\partial \tau^2} = \frac{\varepsilon^2}{1-q}\frac{\partial^2 \pi_1}{\partial z^2} + O(\varepsilon) \tag{29}$$

where, using the mass-weighted coordinates, the non-dimensional sound speed in the external zone is $1/\sqrt{1-q}$ and, according to the isentropic compression $\pi = \theta^{\gamma/(\gamma-1)}$,

$$\theta_{\text{ext+}} = (1-q) + (1-q)\frac{\gamma-1}{\gamma}\varepsilon\pi_1 + O(\varepsilon^2). \tag{30}$$

The second equation in (29) shows that the pressure varies on a length larger than the flame thickness by a factor $1/\varepsilon$ provide the characteristic time is not smaller than the transit time across the laminar flame. Then, it is convenient to introduce the stretched coordinate $z_1 \equiv \varepsilon z$, $\partial/\partial z = \varepsilon\partial/\partial z_1$, writing the pressure field in the form

$$\varepsilon \ll 1, \quad z_1 \equiv \varepsilon z: \quad \pi = 1 + \varepsilon\pi_1(z_1,\tau) + O(\varepsilon^2), \quad \frac{\partial\pi_1(z_1,\tau)}{\partial\tau} = -\frac{1}{\sqrt{1-q}}\frac{\partial\pi_1(z_1,\tau)}{\partial z_1} + O(\varepsilon). \tag{31}$$

This confirms that the pressure variation across the flame structure of order ε^2 is negligible. Moreover, according to (29)–(30), one has

$$\frac{\partial \mathrm{v}_{\text{ext+}}(z_1,\tau)}{\partial z_1} = -\frac{(1-q)}{\gamma}\frac{\partial\pi_1(z_1,\tau)}{\partial\tau} + O(\varepsilon) = \frac{\sqrt{1-q}}{\gamma}\frac{\partial\pi_1(z_1,\tau)}{\partial z_1} + O(\varepsilon), \tag{32}$$

$$\theta_{\text{ext+}}(z_1,\tau) = (1-q) + (1-q)\frac{\gamma-1}{\gamma}\varepsilon\pi_1(z_1,\tau) + O(\varepsilon^2). \tag{33}$$

Integrating (32) from the leading edge of the compression wave where, according to (27), $\pi_1 = 0$ and $\mathrm{v}_{\text{ext+}} = S_i + q$ leads to the external flow velocity in terms of the pressure

$$\mathrm{v}_{\text{ext+}}(z_1,\tau) = S_i + q + \frac{\sqrt{1-q}}{\gamma}\pi_1(z_1,\tau) + O(\varepsilon). \tag{34}$$

3.5.2. *Eigenvalue problem*

Using (31), Equations (15)–(18) written outside the reaction zone takes the form

$$\varepsilon \ll 1: \quad \frac{\partial \mathrm{v}}{\partial z} = [1-\varepsilon\pi_1]\frac{\partial^2\theta}{\partial z^2} - \varepsilon\frac{1}{\gamma}\theta\frac{\partial\pi_1}{\partial\tau} + O(\varepsilon^2) \tag{35}$$

$$\left[\frac{\partial \mathrm{v}}{\partial\tau} - m(\tau)\frac{\partial \mathrm{v}}{\partial z} - \frac{\partial^2 \mathrm{v}}{\partial z^2}\right] = -\frac{1}{\gamma}\frac{\partial\pi_1}{\partial z_1} \tag{36}$$

$$\left[\frac{\partial Y}{\partial\tau} - m(\tau)\frac{\partial Y}{\partial z} - \frac{\partial^2 Y}{\partial z^2}\right] = 0 \tag{37}$$

$$\left[\frac{\partial\theta}{\partial\tau} - m(\tau)\frac{\partial\theta}{\partial z} - \frac{\partial^2\theta}{\partial z^2}\right] = \varepsilon\frac{(\gamma-1)}{\gamma}\theta\frac{\partial\pi_1}{\partial\tau} + O(\varepsilon^2). \tag{38}$$

Equation (35) is obtained from (15) by using (38) to eliminate $\partial\theta/\partial\tau - m\partial\theta/\partial z$. Equations (29)–(30) for the external flow of unburned gas are recovered from (35), (36) and (38) when the second derivative with respect to z (thermal and viscous dissipation) are negligible, as it is the case to leading order in the external flow.

The unsteady term $\varepsilon\theta\,\partial\pi_1/\partial\tau$ on the right-hand side of (35) and (38) describes the small unsteady disturbances of pressure that modify drastically the inner structure of the flame due to the amplification by the large activation energy in the limit (6). The time-dependent mass flux $m(\tau)$, namely the unsteady laminar flame velocity $\mathrm{u}_b(\tau)$ to leading order, is an unknown function (eigenvalue of the problem) obtained by solving (35)–(38) with the boundary conditions (21)–(27), in which the back flow $\mathrm{v}_b(\tau)$ is a functional of $S(\tau)$ and $\mathrm{u}_b(\tau)$. For example, according to (2), one has simply $\mathrm{v}_b(\tau) = S(\tau)\mathrm{u}_b(\tau)$ when the unsteadiness of the burned gas flow is neglected.

4. Matching the inner flame structure with the external flow of cold gas

Thanks to the two length-scale nature of the problem, the downstream-running compression wave in the external flow of unburned gas that is solution to the wave equation (29), can be expressed in terms of the time dependent pressure on the front $1+\varepsilon\pi_P(\tau)$

$$\pi_1(z_1,\tau)=\pi_P(\tau-z_1\sqrt{1-q}) \quad \text{where } \pi_P(\tau)\equiv\pi_1|_{z_1=0}, \tag{39}$$

and $\theta_{\text{ext+}}(z_1,\tau)$ and $\mathrm{v}_{\text{ext+}}(z_1,\tau)$ are given by (33) and (34).

4.1. *Matching the temperature*

Denoting the internal solution by the superscript (i), the unsteady structure of the preheated zone of the flame ($z=O(1)$) is governed by (37)–(38)

$$\left[\frac{\partial Y}{\partial\tau}-m(\tau)\frac{\partial Y}{\partial z}-\frac{\partial^2 Y}{\partial z^2}\right]=0 \tag{40}$$

$$z\geqslant 0: \quad \left[\frac{\partial\theta^{(i)}}{\partial\tau}-m(\tau)\frac{\partial\theta^{(i)}}{\partial z}-\frac{\partial^2\theta^{(i)}}{\partial z^2}\right]=\varepsilon\frac{(\gamma-1)}{\gamma}\theta^{(i)}(z,\tau)\frac{\mathrm{d}\pi_P(\tau)}{\mathrm{d}\tau}+O(\varepsilon^2). \tag{41}$$

The boundary condition at the exit of the preheated zone on the cold gas side ($z=O(1)$, $z\to\infty$: $\lim_{z\to\infty}Y=0$) is obtained by matching the internal temperature with the external solution $\theta_{\text{ext}_+}(z_1,\tau)$

$$\lim_{z\to\infty}\theta^{(i)}(z,\tau)=\theta_{\text{ext}_+}(z_1,\tau)|_{z_1=0}, \quad \lim_{z\to\infty}\partial\theta^{(i)}/\partial z=\varepsilon\partial\theta_{\text{ext}_+}/\partial z_1|_{z_1=0}=O(\varepsilon^2). \tag{42}$$

According to (33), $\partial\theta_{\text{ext}_+}/\partial z_1=O(\varepsilon)$ so that $\lim_{z\to\infty}\partial\theta^{(i)}/\partial z=O(\varepsilon^2)$ is negligible to first order in a perturbation analysis for small ε,

$$\lim_{z\to\infty}\theta^{(i)}(z,\tau)-(1-q)\approx\varepsilon(1-q)\frac{\gamma-1}{\gamma}\pi_P(\tau), \quad \lim_{z\to\infty}\partial\theta^{(i)}/\partial z\approx 0, \quad \lim_{z\to\infty}Y=0. \tag{43}$$

Equations (40)–(41) have to be solved using (43) and the boundary conditions (21)–(23) on the reaction sheet ($z=0$) in the distinguished limit (6). The fully unsteady problem requires the solution in the burned gas side of the reaction sheet $z<0$ to compute $\partial\theta/\partial z|_{z=0^-}$ in the jump condition (23). We will come back to this question later.

4.2. *Matching the flow velocity. Master equation*

Matching the flow velocity in the preheated zone with the external flow of cold gas (34) yields

$$\lim_{z\to\infty}\mathrm{v}^{(i)}(z,\tau)=\mathrm{v}_{\text{ext}_+}(z_1,\tau)|_{z_1=0}=S_i+q+\frac{\sqrt{1-q}}{\gamma}\pi_P(\tau)+O(\varepsilon), \tag{44}$$

$$\lim_{z\to\infty}\frac{\partial\mathrm{v}^{(i)}}{\partial z}=\varepsilon\left.\frac{\partial\mathrm{v}_{\text{ext}_+}}{\partial z_1}\right|_{z_1=0}=-\varepsilon\frac{(1-q)}{\gamma}\frac{\mathrm{d}\pi_P(\tau)}{\mathrm{d}\tau}+O(\varepsilon^2) \tag{45}$$

where (34) has been used. Equations (44)–(45) yield

$$\lim_{z\to\infty}\mathrm{v}^{(i)}(z,\tau)\to S_i+q+\frac{\sqrt{1-q}}{\gamma}\pi_P(\tau)-\varepsilon\, z\,\frac{(1-q)}{\gamma}\frac{\mathrm{d}\pi_P(\tau)}{\mathrm{d}\tau}+O(\varepsilon^2). \tag{46}$$

Integrating (35), written in the form

$$\frac{\partial\mathrm{v}^{(i)}}{\partial z}=[1-\varepsilon\pi_P(\tau)]\frac{\partial^2\theta^{(i)}}{\partial z^2}-\varepsilon\frac{1}{\gamma}[\theta^{(i)}-(1-q)]\frac{\mathrm{d}\pi_P(\tau)}{\mathrm{d}\tau}-\varepsilon(1-q)\frac{1}{\gamma}\frac{\mathrm{d}\pi_P(\tau)}{\mathrm{d}\tau}+O(\varepsilon^2),$$

from the reaction sheet ($z=0:\mathrm{v}^{(i)}=\mathrm{v}_b$) yields the flow velocity in the preheated zone

$$z=O(1):\quad \mathrm{v}^{(i)}(z,\tau)-\mathrm{v}_b(\tau)=[1-\varepsilon\pi_P(\tau)]\left(\frac{\partial\theta^{(i)}}{\partial z}-\frac{\partial\theta^{(i)}}{\partial z}\bigg|_{z=0^+}\right)$$
$$-\varepsilon\frac{1}{\gamma}\frac{\mathrm{d}\pi_P(\tau)}{\mathrm{d}\tau}\int_0^z[\theta^{(i)}-(1-q)]\mathrm{d}z-\varepsilon\, z\,(1-q)\frac{1}{\gamma}\frac{\mathrm{d}\pi_u(\tau)}{\mathrm{d}\tau}+O(\varepsilon^2). \quad (47)$$

Thanks to (43) $\lim_{z\to\infty}\theta^{(i)}(z,\tau)=(1-q)+O(\varepsilon)$, the leading order of the integral on the right-hand side of (47) is well defined in the limit $z\to\infty$ and is of order unity. Then, using (46), the limit $z\to\infty$ of (47) yields

$$\mathrm{v}_b(\tau)-\left[S_i+q+\frac{\sqrt{1-q}}{\gamma}\pi_P(\tau)\right]=[1-\varepsilon\pi_P(\tau)]\left.\frac{\partial\theta^{(i)}}{\partial z}\right|_{z=0^+}$$
$$+\varepsilon\frac{1}{\gamma}\frac{\mathrm{d}\pi_P(\tau)}{\mathrm{d}\tau}\int_0^{+\infty}[\theta^{(i)}-(1-q)]\mathrm{d}z+O(\varepsilon^2). \quad (48)$$

where the thermal flux out of the reaction sheet $\partial\theta^{(i)}/\partial z|_{z=0^+}$ is obtained in terms of the flame temperature θ_b by the jump condition (22). The integral term on the right-hand side of (48) which is meaningful as soon as $\mathrm{d}\pi_P(\tau)/\mathrm{d}\tau<\varepsilon$ is indeed not useful for the leading order of the flow. Using the jump relation (22), the leading order of Equation (48) takes the form

$$\mathrm{v}_b(\tau)-\left[S_i+q+\frac{\sqrt{1-q}}{\gamma}\pi_P(\tau)\right]=-q\exp\left(\frac{\beta}{2}[\theta_b(\tau)-1]\right)+O(\varepsilon). \quad (49)$$

valid for the ZFK model without restriction concerning the characteristic time of the dynamics. When the inner structure of the flame is in steady state, using the ZFK result for the ratio of laminar flame velocity $\mathrm{u}_b\equiv U_b(T_b)/U_b(T_{bi})=\mathrm{e}^{\beta(\theta_b-1)/2}$ on the right-hand side, Equation (49) reduces to the well known relation between the flows just upstream and downstream a steady planar flame, u_u in the unburned and u_b in the burned gas, $u_u-u_b=[T_b/T_u-1]U_b$. Equation (49) is the *master equation* used in the nonlinear dynamics of the flame front.

5. Quasi-steady solutions

Before considering the full dynamics, it is worth studying the dynamics of the quasi-steady solutions (inner structure of the flame and burned gas flow assumed in steady state). The results are not expected to be different from those obtained when the flame was considered as a discontinuity [18]. The flame structure of the quasi-steady solutions denoted by an overbar, is obtained by neglecting the unsteady terms in (40)–(41)

$$-\overline{m}(\tau)\frac{\partial\overline{Y}}{\partial z}-\frac{\partial^2\overline{Y}}{\partial z^2}=0 \quad (50)$$

$$z\geqslant 0:\quad -\overline{m}(\tau)\frac{\partial\overline{\theta}^{(i)}}{\partial z}-\frac{\partial^2\overline{\theta}^{(i)}}{\partial z^2}=O(\varepsilon^2). \quad (51)$$

Introducing the short notation

$$\overline{\theta}_u(\tau)\equiv(1-q)\left[1+\varepsilon\frac{\gamma-1}{\gamma}\overline{\pi}_P(\tau)\right], \quad (52)$$

for the gas temperature just ahead of the flame as it is modified by the downstream running acoustic wave in the unburned gas flow, the quasi-steady solution satisfying the boundary condition (43) reads

$$z\geqslant 0:\quad \overline{Y}=\mathrm{e}^{-\overline{m}(\tau)z},\quad \overline{\theta}^{(i)}(z,\tau)=\left[\overline{\theta}_b(\tau)-\overline{\theta}_u(\tau)\right]\mathrm{e}^{-\overline{m}z}+\overline{\theta}_u(\tau),$$
$$z\leqslant 0:\quad \overline{Y}=1,\qquad \overline{\theta}^{(i)}=\overline{\theta}_b(\tau). \quad (53)$$

Then, the boundary conditions on the reaction sheet (22)–(23) determine the solution. The flame temperature $\overline{\theta}_b(\tau)$ is obtained from (23) with $\partial\theta/\partial z|_{z=0^-} = 0$ and the laminar flame velocity $\overline{m}(\tau) \approx \overline{\mathrm{u}}_b$ given by (22) corresponds to the ZFK solution $\overline{\mathrm{u}}_b = \mathrm{e}^{\beta(\overline{\theta}_b-1)/2}$. Expressed in terms of the pressure $\overline{\pi}_P(\tau)$, the steady state solution reads

$$\overline{\theta}_b(\tau) = \overline{\theta}_u(\tau) + q, \quad \overline{\theta}_b(\tau) - 1 = \varepsilon(1-q)\frac{\gamma-1}{\gamma}\overline{\pi}_P(\tau) + O(\varepsilon^2), \tag{54}$$

$$\beta(\overline{\theta}_b - 1)/2 = \beta\left[\overline{\theta}_u(\tau) + q - 1\right]/2 = b\overline{\pi}_P(\tau), \quad \overline{m}(\tau) = \mathrm{e}^{b\overline{\pi}_P(\tau)} + O(1/\beta), \quad b \equiv \frac{\beta\varepsilon}{2}\frac{(\gamma-1)}{\gamma}(1-q) \tag{55}$$

where the parameter b (not to be confused with the subscript b) is of order unity in the limit (6).

5.1. *Turning point of the quasi-steady solutions (saddle-node bifurcation)*

In the quasi-steady state approximation, the back-flow is (2) $\mathrm{v}_b(\tau) = S(\tau)\,\overline{m}(\tau)$ to give using (55)

$$\overline{\mathrm{v}}_b(\tau) = S(\tau)\,\overline{m}(\tau) = S(\tau)\,\mathrm{e}^{b\overline{\pi}_P(\tau)}, \quad b \equiv \frac{\beta\varepsilon}{2}\frac{(\gamma-1)}{\gamma}S_i. \tag{56}$$

Introducing (56) into the master Equation (49), the same transcendental equation as in [18] is obtained, yielding the pressure $\overline{\pi}_P$ in terms of the flame elongation $S(\tau)$

$$(S+q)\mathrm{e}^{b\overline{\pi}_P} = (S_i+q) + \frac{\sqrt{1-q}}{\gamma}\overline{\pi}_P. \tag{57}$$

The pressure and the flame temperature $\overline{\pi}_P$ and $\overline{\theta}_b$ depend on the time only through the elongation S. Introducing the notation ϑ and ζ for the rescaled pressure and elongation

$$\vartheta \equiv b\pi_P = O(1), \quad \zeta \equiv S+q, \quad \zeta(\tau) = (1+\epsilon\tau)S_i + q, \tag{58}$$

$$\mathrm{b} \equiv b\gamma/\sqrt{1-q} = (\beta\varepsilon/2)(\gamma-1)\sqrt{1-q} = O(1/S_i), \tag{59}$$

Equation (57) takes the form

$$\zeta\,\mathrm{e}^{\overline{\vartheta}} - \zeta_i - \overline{\vartheta}/\mathrm{b} = 0; \quad \tau = 0: \quad \zeta = \zeta_i \equiv S_i + q, \quad \vartheta = 0. \tag{60}$$

The solution *pressure versus elongation* $\overline{\vartheta}(\zeta)$ depends on the initial elongation ζ_i and involves a single parameter b in (59). The graph of the inverse function $\zeta(\overline{\vartheta})$ is a bell-shaped curve sketched in thick black line in Figure 3. The maximum $\zeta = \zeta^*$, $\overline{\vartheta} = \vartheta^*$ corresponds to

$$\left.\frac{\mathrm{d}\zeta}{\mathrm{d}\overline{\vartheta}}\right|_{\overline{\vartheta}=\vartheta^*} = 0: \quad \zeta^*\mathrm{e}^{\vartheta^*} = \frac{1}{\mathrm{b}}, \quad \vartheta^* = 1 - \zeta_i\,\mathrm{b} > 0, \quad \frac{\zeta^*}{\zeta_i} = \frac{\mathrm{e}^{(\mathrm{b}\zeta_i - 1)}}{\mathrm{b}\zeta_i} \geqslant 1, \tag{61}$$

the inequality $\zeta^*/\zeta_i \geqslant 1$ following from the ordering $0 < \mathrm{b}\zeta_i \leqslant 1$ valid for all reactive gaseous mixtures [18]. The dynamics of the flame is represented by the C-shaped curve $\overline{\vartheta}(\zeta)$ with a turning point at the critical elongation S^*, $\zeta^* = S^* + q$, $\mathrm{d}\overline{\vartheta}/\mathrm{d}\zeta|_{\zeta=\zeta^*} = \infty$. There is no more solution to (60) for $\zeta > \zeta^*$ and there are two branches of solutions for $\zeta < \zeta^*$, $\overline{\vartheta}_\pm = \vartheta^* \pm \sqrt{2(\zeta^*-\zeta)/\zeta^*}$, $\overline{\vartheta}_- - \vartheta^* < 0 < \overline{\vartheta}_+ - \vartheta^*$, $\mathrm{d}\overline{\vartheta}_-/\mathrm{d}\zeta > 0$ and $\mathrm{d}\overline{\vartheta}_+/\mathrm{d}\zeta < 0$, see Figure 3. The physical branch is $\overline{\vartheta}_-(\zeta)$ for which the flame temperature increases with the flame acceleration on the tip $\mathrm{d}\zeta/\mathrm{d}\tau = \epsilon S_i$ since $\mathrm{d}\overline{\vartheta}_-/\mathrm{d}(\epsilon S_i) = \tau\mathrm{d}\overline{\vartheta}_-/\mathrm{d}\zeta > 0$. As previously mentioned [18], an initial elongation close to the upper bound $\zeta_i = \zeta^*$, $S = S^*_{\max}$ corresponds to a universal critical Mach number $2/[\beta(\gamma-1)]$ of the unburned gas flow adjacent to the flame. According to (60)–(61), this critical flow Mach number is close to unity while the critical laminar flame velocity remains markedly subsonic $U_b^*/a_b^* \approx 0.05$, in good agreement with the pre-conditioned state in the DDT onset of the 2010 experiments and numerics [11, 12].

5.2. *Finite-time singularity of the quasi-steady dynamics*

Equations (57) and (61) are relevant if the response of the flame structure to a change in elongation is quasi-instantaneous. A necessary condition is that the rate of elongation is smaller that the inverse of the transit time in (5)

$$\epsilon \ll 1. \tag{62}$$

Then, according to (5) $\mathrm{d}\zeta/\mathrm{d}\tau = \epsilon S_i$, $\epsilon \ll 1$, the laminar flame velocity of the quasi-steady solutions $\overline{m} = \mathrm{e}^{\overline{\vartheta}}$ ($\overline{\vartheta} \equiv b\overline{\pi}_P$) increase first slowly with the time $\mathrm{d}\overline{m}/\mathrm{d}\tau = O(\epsilon S_i)$, but, according to (61), the flame acceleration diverges abruptly when the elongation reaches its critical value S^* $\mathrm{d}\overline{m}/\mathrm{d}\tau|_{\tau=\tau^*} = \epsilon S_i \overline{m}^* \mathrm{d}\overline{\vartheta}/\mathrm{d}\zeta|_{\zeta=\zeta^*} = \infty$ since $\mathrm{d}\overline{\vartheta}/\mathrm{d}\zeta|_{\zeta=\zeta^*} = \infty$ (turning point). This finite-time singularity of the flame acceleration occurs for a critical laminar flame velocity U_b^* markedly subsonic $\overline{m}^* = \mathrm{e}^{\vartheta^*}$ where $0 < \vartheta^* = (1-\zeta_i \mathrm{b}) < 1$, $U_b^*/a_b^* = O(\varepsilon)$. As when the flame is treated as a discontinuity [6], Equation (60) takes a generic form near the critical point $\mathrm{d}\zeta/\mathrm{d}\overline{\vartheta}|_{\overline{\vartheta}=\vartheta^*} = 0$,

$$\left.\frac{\mathrm{d}^2\zeta}{\mathrm{d}\vartheta^2}\right|_{\vartheta=\vartheta^*} = -\zeta^* \quad \Rightarrow \quad \frac{\zeta^*-\zeta}{\zeta^*} \ll 1: \quad \frac{\zeta^*-\zeta}{\zeta^*} \approx \frac{1}{2}(\vartheta^*-\overline{\vartheta})^2 \tag{63}$$

obtained by a Taylor expansion. Using (5), the quasi-steady dynamics of the flame pressure near the critical condition $\tau = \tau^*$ takes the form

$$\tau^* - \tau \to 0^+: \quad \vartheta^* - \overline{\vartheta}_-(\tau) \approx \kappa\sqrt{\tau^*-\tau} \quad \text{where } \kappa \equiv \sqrt{2\epsilon\frac{S_i}{S^*+q}} = O(\sqrt{\epsilon}), \tag{64}$$

exhibiting the finite-time singularity of the flame acceleration of the physical branch of solutions

$$\frac{\mathrm{d}\overline{\vartheta}_-}{\mathrm{d}\tau} \approx \frac{\kappa/2}{\sqrt{\tau^*-\tau}}, \quad \frac{\mathrm{d}\overline{\pi}_P}{\mathrm{d}\tau} \approx \frac{\kappa/2b}{\sqrt{\tau^*-\tau}}, \quad \frac{1}{\overline{m}}\frac{\mathrm{d}\overline{m}}{\mathrm{d}\tau} \approx \frac{\kappa/2}{\sqrt{\tau^*-\tau}}. \tag{65}$$

According to (31)–(32) and (39), the gradient of the external unburned flow also diverges on the flame,

$$\tau^* - \tau \to 0^+: \quad \left.\frac{\partial \mathrm{v}_{\mathrm{ext}_+}}{\partial z_1}\right|_{z_1=0} \approx \frac{(1-q)}{\gamma}\frac{\kappa/2}{b}\frac{1}{\sqrt{\tau^*-\tau}}, \quad \left.\frac{\partial \mathrm{v}_{\mathrm{ext}_+}}{\partial \tau}\right|_{z_1=0} \approx \frac{\sqrt{1-q}}{\gamma}\frac{\kappa/2}{b}\frac{1}{\sqrt{\tau^*-\tau}}. \tag{66}$$

The finite-time singularity (66) corresponds to a break down of the quasi-steady dynamics so that the quasi-steady solutions are no longer valid near the turning point even for a slow elongation (62). Moreover, the physical branch of quasi-steady solutions $\overline{\vartheta}_-(\zeta)$ should be stable to be meaningful for the unsteady solutions when the elongation $\zeta(\tau)$ increases slowly $\epsilon \ll 1$. These problems are addressed in the following sections.

6. Linear stability of the quasi-steady solutions

The stability analysis is performed from the linearized version of the master equation (49) yielding the relation between for $\delta\pi_P \equiv \pi_P - \overline{\pi}_P$, $\delta \mathrm{v}_b \equiv \mathrm{v}_b - \overline{\mathrm{v}}_b$ and $\delta\theta_b \equiv \mathrm{v}_b - \overline{\theta}_b$

$$\overline{\mathrm{v}}_b - \left[S_i + q + \frac{\sqrt{1-q}}{\gamma}\overline{\pi}_P(\tau)\right] = -q\overline{m}, \quad \text{where } \overline{m} = \exp\left(\frac{\beta}{2}\left[\overline{\theta}_b(\tau)-1\right]\right) \text{ and } \overline{\mathrm{v}}_b = S\overline{m} \tag{67}$$

$$\delta \mathrm{v}_b - \frac{\sqrt{1-q}}{\gamma}\delta\pi_P = -\frac{q}{2}\overline{m}\,\delta\theta_{b1} \quad \text{where } \theta_{b1} \equiv \beta(\theta_b - 1)\,] = O(1). \tag{68}$$

The linear stability of the quasi-steady solutions involves the linear variation of the flame temperature with the pressure for a fixed elongation $S \leqslant S^*$ ($\overline{m}$ and $\overline{\pi}_P$ fixed)

$$\delta \mathrm{v}_b|_{S=\mathrm{cst.}} - \frac{\sqrt{1-q}}{\gamma}\delta\pi_P = -\frac{q}{2}\overline{m}\,\delta\theta_{b1}|_{S=\mathrm{cst.}}. \tag{69}$$

Looking for a solution in the form

$$\delta\pi_P(\tau)=e^{\sigma\tau}\tilde{\pi}_P(\sigma),\quad \delta v_b|_{S=cst.}(\tau)=e^{\sigma\tau}\tilde{v}_b(\sigma),\quad \delta\theta_{b1}|_{S=cst.}(\tau)=e^{\sigma\tau}\tilde{\theta}_{b1}(\sigma) \tag{70}$$

an equation for the complex growth rate σ is obtained when $\tilde{v}_b(\sigma)$ and $\tilde{\theta}_{b1}(\sigma)$ are expressed linearly in term of $\tilde{\pi}_P(\sigma)$. The quasi-steady solution is unstable (stable) if Re(σ)>0 (Re(σ)<0). The linear response of a steady planar flame subjected to a uniform pressure fluctuation should be performed in a first step.

6.1. *Linear response to a pressure fluctuation*

Introducing the short notation $f(\tau)\equiv\beta\varepsilon[(\gamma-1)/\gamma]\pi_P(\tau)$ for the reduced pressure $p(\tau)/p_i=1+\varepsilon\pi_P(\tau)$ (forcing term) and working in the limit $\beta\gg1$ with the distinguished limit (6), $\beta\varepsilon=O(1)$, Equations (40)–(41) governing the flame structure outside the reaction sheet take the form

$$\left[\frac{\partial Y}{\partial\tau}-m(\tau)\frac{\partial Y}{\partial z}-\frac{\partial Y}{\partial z^2}\right]=0,\quad Y(z,\tau)\in[0,1] \tag{71}$$

$$\left[\frac{\partial\theta}{\partial\tau}-m(\tau)\frac{\partial\theta}{\partial z}-\frac{\partial^2\theta}{\partial z^2}\right]=\frac{\theta}{\beta}\frac{df}{d\tau},\quad f(\tau)\equiv\beta\varepsilon[(\gamma-1)/\gamma]\pi_P(\tau), \tag{72}$$

where the superscript (i) is suppressed for saving the notation. The problem is solved in the limit $\beta\to\infty$ using the boundary conditions (21)–(23) on the reaction zone and at infinity in both preheated zone ($z\geqslant0$) and burned gas ($z<0$)

$$z\to\infty:\quad \theta\to(1-q)+\frac{(1-q)}{\beta}f(\tau),\quad Y\to0, \tag{73}$$

$$z\leqslant0:\quad Y=1,\quad z\to-\infty:\quad \theta\to1+\frac{1}{\beta}f(\tau), \tag{74}$$

expressing that the compressional heating is adiabatic and uniform far away from the flame on both sides (hot burned gas and cold unburned gas) $\delta T/\overline{T}=[(\gamma-1)/\gamma]\delta T/\overline{T}$. The problem consists in determining the disturbances of reduced mass flux and flame temperature $\delta m(\tau)$ and $\delta(\beta[\theta_b(\tau)-1])$ for a given time dependent pressure fluctuation $\delta f(\tau)$. According to the asymptotic method for large β, one introduces the decomposition,

$$\theta=\theta_0+\frac{\theta_1}{\beta},\quad \theta_b=1+\frac{\theta_{b1}}{\beta},\quad Y=Y_0+\frac{Y_1}{\beta},\quad m=m_0+\frac{m_1}{\beta} \tag{75}$$

and, according to (22)–(23) and (73)–(74),

$$z\to\infty:\quad \theta_0\to(1-q);\quad z\to-\infty:\quad \theta_0\to1 \tag{76}$$

$$\left.\frac{\partial\theta_0}{\partial z}\right|_{z=0^+}=-q\exp(\theta_{b1}/2),\quad \left.\frac{\partial\theta_{0,1}}{\partial z}\right|_{z=0^-}=\left.\frac{\partial\theta_{0,1}}{\partial z}\right|_{z=0^+}-q\left.\frac{\partial Y_{0,1}}{\partial z}\right|_{z=0^+}, \tag{77}$$

and the temperature should be solved up to the first order in the $1/\beta$ expansion. In the linear response one considers $\delta f(\tau)\ll1$ and looks for the linear perturbations $\delta\theta(z,\tau)$ and $\delta Y(z,\tau)$

$$f=\overline{f}+\delta f,\quad \theta=\overline{\theta}+\delta\theta,\quad Y=\overline{Y}+\delta Y. \tag{78}$$

The unperturbed solution is a steady state solution in (52)–(55) $\overline{\beta}[\overline{\theta}_b-1]=(1-q)\overline{f}$, $\overline{m}=e^{(1-q)\overline{f}/2}$

$$z>0:\quad \overline{\theta}=qe^{-\overline{m}z}+(1-q)+\frac{(1-q)}{\beta}\overline{f},\quad Y=e^{-\overline{m}z};\quad z<0:\quad \overline{\theta}=\overline{\theta}_b=1+\frac{(1-q)}{\beta}\overline{f},\quad \overline{Y}=1. \tag{79}$$

The linear Equations (71)–(72) in the preheated zone read

$$z \geqslant 0: \quad \left[\frac{\partial \delta Y}{\partial \tau} - \overline{m}\frac{\partial \delta Y}{\partial z} - \frac{\partial^2 \delta Y}{\partial z^2}\right] = -\delta m\, \overline{m}\, \mathrm{e}^{-\overline{m} z}, \tag{80}$$

$$\left[\frac{\partial \delta\theta}{\partial \tau} - \overline{m}\frac{\partial \delta\theta}{\partial z} - \frac{\partial^2 \delta\theta}{\partial z^2}\right] = -q\,\delta m\, \overline{m}\, \mathrm{e}^{-\overline{m} z} + \frac{\overline{\theta}(z)}{\beta}\frac{\mathrm{d}\delta f}{\mathrm{d}\tau}, \tag{81}$$

$$z \to \infty: \quad \delta\theta = \frac{(1-q)}{\beta}\delta f, \quad \delta Y = 0; \quad z = 0: \quad \delta\theta = \frac{\delta\theta_{b1}}{\beta}, \quad \delta Y = 0. \tag{82}$$

where the unknown fluctuations of flame temperature $\beta(\theta_b - \overline{\theta}_b) \equiv \delta\theta_{b1}(\tau)$ and mass flux $\delta m(\tau)$ are eigenvalues. The solution is obtained in Fourier transform. Considering a harmonic pressure disturbance $\delta f(\tau) = \mathrm{e}^{\mathrm{i}\omega\tau}\tilde{f}(\omega)$, the solution is looked for in the form $\delta m(\tau) = \mathrm{e}^{\mathrm{i}\omega\tau}\tilde{m}(\omega)$, $\delta\theta(z,\tau) = \mathrm{e}^{\mathrm{i}\omega\tau}\tilde{\theta}(z,\omega)$, $\delta Y(z,\tau) = \mathrm{e}^{\mathrm{i}\omega\tau}\tilde{Y}(z,\omega)$. To leading in the asymptotic limit $\beta \gg 1$, the linear equations in the preheated zone take the form

$$z \geqslant 0: \quad \left[\mathrm{i}\omega\tilde{Y}_0 - \overline{m}\frac{\mathrm{d}\tilde{Y}_0}{\mathrm{d}z} - \frac{\mathrm{d}^2\tilde{Y}_0}{\mathrm{d}z^2}\right] = -\tilde{m}_0\, \overline{m}\, \mathrm{e}^{-\overline{m} z}, \tag{83}$$

$$\left[\mathrm{i}\omega\tilde{\theta}_0 - \overline{m}\frac{\mathrm{d}\tilde{\theta}_0}{\mathrm{d}z} - \frac{\mathrm{d}^2\tilde{\theta}_0}{\mathrm{d}z^2}\right] = -q\,\tilde{m}_0\, \overline{m}\, \mathrm{e}^{-\overline{m} z}, \tag{84}$$

$$z \to \infty: \quad \tilde{\theta}_0 = 0, \quad \tilde{Y}_0 = 0; \quad z = 0: \quad \tilde{\theta}_0 = 0, \quad \tilde{Y}_0 = 0. \tag{85}$$

Introducing the notation $\kappa_\pm(\omega) \equiv \overline{m}[-1 \pm \sqrt{1 + 4\mathrm{i}\omega/\overline{m}^2}]/2$, $\mathrm{Re}(\kappa_+) > 0$, $\mathrm{Re}(\kappa_-) < 0$, the general solutions of (83)–(84) takes the general form

$$z \geqslant 0: \quad \tilde{\theta}_0(z,\omega) = A_-\mathrm{e}^{\kappa_- z} + A_+\mathrm{e}^{\kappa_+ z} + \frac{1}{\kappa_- - \kappa_+}\left[\frac{\mathrm{e}^{-\overline{m} z} - \mathrm{e}^{\kappa_+ z}}{\overline{m} + \kappa_+} - \frac{\mathrm{e}^{-\overline{m} z} - \mathrm{e}^{\kappa_- z}}{\overline{m} + \kappa_-}\right] q\,\overline{m}\,\tilde{m}_0, \tag{86}$$

where $A_\pm(\omega)$ are constants of integration determined by the boundary conditions. According to the boundary condition in the unburned gas, elimination of the divergence for $z \to \infty$ yields $A_+ = [(\kappa_- - \kappa_+)(\overline{m} + \kappa_+)]^{-1} q\overline{m}\,\tilde{m}_0$ and $A_- = \tilde{\theta}_0(0) - A_+$ to satisfy $\tilde{\theta}_0(0) = 0$ ($\delta\theta = O(1/\beta)$),

$$q\tilde{Y}_0 = \tilde{\theta}_0 = \frac{\mathrm{e}^{-\overline{m} z} - \mathrm{e}^{\kappa_- z}}{(\overline{m} + \kappa_+)(\overline{m} + \kappa_-)}\, q\,\overline{m}\,\tilde{m}_0, \quad \left.\frac{\mathrm{d}\tilde{\theta}_0}{\mathrm{d}z}\right|_{z=0^+} = -\frac{1}{\overline{m} + \kappa^+}\, q\,\overline{m}\,\tilde{m}_0. \tag{87}$$

The first jump condition (77) $\mathrm{d}\tilde{\theta}_0/\mathrm{d}z|_{z=0^+} = -q\overline{m}\tilde{\theta}_{b1}/2$ yields

$$\tilde{m}_0(\omega) = \frac{[\overline{m} + \kappa^+(\omega)]}{2}\tilde{\theta}_{b1}(\omega). \tag{88}$$

The $1/\beta$-modification to the flame temperature $\tilde{\theta}_{b1}(\omega)$ is obtained by solving the first order in the $1/\beta$ expansion of the linear Equations (80)–(82)

$$z \geqslant 0: \quad \left[\mathrm{i}\omega\tilde{Y}_1 - \overline{m}\frac{\mathrm{d}\tilde{Y}_1}{\mathrm{d}z} - \frac{\mathrm{d}^2\tilde{Y}_1}{\mathrm{d}z^2}\right] = -\tilde{m}_1(\omega)\overline{m}\,\mathrm{e}^{-\overline{m} z}, \tag{89}$$

$$\left[\mathrm{i}\omega\tilde{\theta}_1 - \overline{m}\frac{\mathrm{d}\tilde{\theta}_1}{\mathrm{d}z} - \frac{\mathrm{d}^2\tilde{\theta}_1}{\mathrm{d}z^2}\right] = -q\,\tilde{m}_1(\omega)\overline{m}\,\mathrm{e}^{-\overline{m} z} + [q\mathrm{e}^{-\overline{m} z} + (1-q)]\mathrm{i}\omega\tilde{f}, \tag{90}$$

$$z \to \infty: \quad \delta\theta_1 = (1-q)\delta f, \quad \delta Y_1 = 0; \quad z = 0: \quad \delta\theta_1 = \theta_{b1}, \quad \delta Y_1 = 0. \tag{91}$$

Elimination of $\tilde{m}_1(\omega)$ by considering $\tilde{Z}_1(z,\omega) \equiv \tilde{\theta}_1(z,\omega) - (1-q)\tilde{f} - q\tilde{Y}_1(z,\omega)$ yields

$$\frac{\mathrm{d}^2\tilde{Z}_1}{\mathrm{d}z^2} + \overline{m}\frac{\mathrm{d}\tilde{Z}_1}{\mathrm{d}z} - \mathrm{i}\omega\tilde{Z}_1 = -q\mathrm{e}^{-\overline{m} z}\mathrm{i}\omega\tilde{f} \tag{92}$$

$$z \to \infty: \quad \tilde{Z}_1 = 0; \quad z = 0: \quad \tilde{Z}_1 = \tilde{\theta}_{b1}(\omega) - (1-q)\tilde{f}. \tag{93}$$

The solution of (92) satisfying the boundary condition (93) is expressed in terms of $\tilde{\theta}_{b1}(\omega)$

$$z \geqslant 0: \qquad \tilde{Z}_1 = [\tilde{\theta}_{b1} - (1-q)\tilde{f}]\mathrm{e}^{\kappa_- z} - \frac{\mathrm{e}^{-\overline{m}z} - \mathrm{e}^{\kappa_- z}}{(\overline{m}+\kappa_+)(\overline{m}+\kappa_-)} q\,\mathrm{i}\omega\tilde{f} \tag{94}$$

$$\left.\frac{\mathrm{d}\tilde{Z}_1}{\mathrm{d}z}\right|_{z=0^+} = \left.\frac{\mathrm{d}(\tilde{\theta}_1 - q\tilde{Y}_1)}{\mathrm{d}z}\right|_{z=0^+} = \kappa_-[\tilde{\theta}_{b1} - (1-q)\tilde{f}] + \frac{q\,\mathrm{i}\omega\tilde{f}}{\overline{m}+\kappa_+}. \tag{95}$$

The second jump condition in (77),

$$\left.\frac{\mathrm{d}\tilde{\theta}_1}{\mathrm{d}z}\right|_{z=0^-} = \kappa_-[\tilde{\theta}_{b1} - (1-q)\tilde{f}] + \frac{q\,\mathrm{i}\omega\tilde{f}}{\overline{m}+\kappa_+} \tag{96}$$

yields the perturbation of the flame temperature $\tilde{\theta}_{b1}(\omega)$ in terms of the pressure fluctuation $\tilde{f}(\omega)$ when the solution for $\tilde{\theta}_1(z,\omega)$ is known in the burned gas flow ($z<0$). Using (79) $\overline{\theta}_0 = 1$ ($\tilde{\theta}_0 = 0$) in the burned gas, the linearized version of Equation (72) and the boundary condition (74) read

$$z \leqslant 0: \quad \frac{\mathrm{d}^2\tilde{\theta}_1}{\mathrm{d}z^2} + \overline{m}\frac{\mathrm{d}\tilde{\theta}_1}{\mathrm{d}z} - \mathrm{i}\omega\tilde{\theta}_1 = -\mathrm{i}\omega\tilde{f} \quad z\to-\infty: \quad \tilde{\theta}_1 \to \tilde{f}; \quad z=0: \quad \tilde{\theta}_1 = \tilde{\theta}_{b1}. \tag{97}$$

The solution yields the temperature fluctuation in the burned gas (of order $1/\beta$)

$$z \leqslant 0: \quad \tilde{\theta}_1(z,\omega) = \tilde{f}(\omega) + (\tilde{\theta}_{b1} - \tilde{f})\,\mathrm{e}^{\kappa_+ z}, \quad \left.\frac{\mathrm{d}\tilde{\theta}_1}{\mathrm{d}z}\right|_{z=0^-} = \kappa_+[\tilde{\theta}_{b1} - \tilde{f}]. \tag{98}$$

The fluctuation of flame temperature is then given in terms of the pressure fluctuation by (96)

$$(\kappa_+ - \kappa_-)[\tilde{\theta}_{b1} - \tilde{f}] = q\kappa_-\tilde{f} + q\frac{\mathrm{i}\omega\tilde{f}}{\overline{m}+\kappa_+} \tag{99}$$

$$\tilde{\theta}_{b1}(\omega) = \tilde{f}(\omega) + \frac{q/\overline{m}}{\sqrt{1+\frac{4\mathrm{i}\omega}{\overline{m}^2}}}\left[-\frac{1+\sqrt{1+\frac{4\mathrm{i}\omega}{\overline{m}^2}}}{2}\overline{m} + \frac{2/\overline{m}}{1+\sqrt{1+\frac{4\mathrm{i}\omega}{\overline{m}^2}}}\mathrm{i}\omega\right]\tilde{f}(\omega) \tag{100}$$

$$\lim_{\omega\to 0}\tilde{\theta}_{b1} = (1-q)\tilde{f} + 2q\frac{\mathrm{i}\omega}{\overline{m}^2}\tilde{f} + O(\omega^2). \tag{101}$$

According to (100), the fluctuation of flame temperature is proportional to the pressure if the heat release is zero (no gas expansion across the flame) $\lim_{q\to 0}\delta\theta_b = \delta f$ as it should be (uniform compressional heating). The fluctuation of the laminar flame velocity obtained from (88) is

$$\tilde{m}_0(\omega) = [\overline{m} + \kappa_+(\omega)]\frac{\tilde{\theta}_{b1}(\omega)}{2}, \quad \lim_{\omega\to 0}\tilde{m}_0(\omega) = \frac{1-q}{2}\overline{m}\left[\tilde{f} + \frac{1+q}{1-q}\frac{\mathrm{i}\omega}{\overline{m}^2}\tilde{f} + O(\omega^2)\right] \tag{102}$$

in agreement with (4.7) in [19]. Back to the original variable, the solution for a slowly varying pressure obtained from (101)–(102) takes the form

$$\frac{1}{\overline{f}}\frac{\mathrm{d}f}{\mathrm{d}\tau} \ll 1: \qquad \delta\theta_{b1}(\tau) = (1-q)\left[f(\tau) + \Delta\tau_\theta\frac{\partial f}{\partial\tau} + \cdots\right], \quad \Delta\tau_\theta = \frac{2q}{(1-q)}\frac{1}{\overline{m}^2}, \tag{103}$$

$$\frac{\delta m_0(\tau)}{\overline{m}} = \frac{1-q}{2}\left[f(\tau) + \Delta\tau_m\frac{\partial f}{\partial\tau} + \cdots\right], \quad \Delta\tau_m = \frac{(1+q)}{(1-q)}\frac{1}{\overline{m}^2}. \tag{104}$$

According to the ZFK solution (55) $\delta\overline{m}/\overline{m} = \delta\overline{\theta}_{b1}/2$, the first terms on the right-hand side of (103) and (104) correspond to the change in flame temperature and laminar flame velocity on the branch of the physical quasi-steady solutions when the pressure is modified, $\delta\overline{\theta}_{b1} = (1-q)\delta f$, $\delta\overline{m}/\overline{m} = (1-q)\delta f/2$. Unsteady modifications to the inner flame structure are described by the following terms that are proportional to the time derivative of the pressure. The variation of flame temperature $\beta(\theta_b - \overline{\theta}_b)$ in (100) in the first Equation (102), relative to its quasi-steady modification, can be conveniently rewritten as

$$\tilde{\theta}_{b1}(\omega) - (1-q)\tilde{f} = q\tilde{\mathscr{Y}}(\mathrm{i}\omega)\frac{4\mathrm{i}\omega}{\overline{m}^2}\tilde{f}, \quad \tilde{\mathscr{Y}}(\mathrm{i}\omega) \equiv \frac{1}{\sqrt{1+4\mathrm{i}\omega/\overline{m}^2}}\frac{1}{\left[1+\sqrt{1+4\mathrm{i}\omega/\overline{m}^2}\right]}, \tag{105}$$

where $\lim_{\omega\to 0}\tilde{\mathscr{Y}} = 1/2$ to give the time dependent flame temperature in the form

$$\delta\theta_{b1}(\tau) - (1-q)\delta f(\tau) = \frac{4}{\overline{m}^2} q \int_{-\infty}^{+\infty} \mathrm{d}\tau' \mathscr{Y}(\tau-\tau') \frac{\partial \delta f(\tau')}{\partial \tau'}. \tag{106}$$

Equation (106) satisfies the principe of causality for a linear response to the time derivative of the pressure (forcing term). This is not the case for the link of the flame temperature (or the laminar flame velocity) with the instantaneous pressure since Equations (103)–(104) can be interpreted as the first term of an expansion in powers of $(1/f)\mathrm{d}f(\tau)/\mathrm{d}\tau$ of the flame temperature and laminar flame velocity, $\delta\theta(\tau) \approx (1-q)f(\tau+\Delta\tau_\theta)+\cdots$, $\delta m(\tau)/\overline{m} \approx [(1-q)/2]f(\tau+\Delta\tau_m)+\cdots$ at a later time ($\Delta\tau_\theta > 0$ for the flame temperature and $\Delta\tau_m > 0$ for the laminar flame velocity). This promotes an instability of the physical branch of quasi-steady solutions presented now.

6.2. *Instability mechanism*

The instability mechanism of the quasi-steady solutions for S fixed is illustrated when the unsteadiness of the burned gas flow is neglected leading to the same expression for the instantaneous back-flow as in (56) for the quasi-steady solutions

$$\mathrm{v}_b = S\,m, \quad \delta\mathrm{v}_b|_{S=\mathrm{cst.}} = S\,\delta m|_{S=\mathrm{cst.}}. \tag{107}$$

Using (107) and the same notation as in (72) $\delta f = \beta\varepsilon[(\gamma-1)/\gamma]\delta\pi_P(\tau)$, Equation (69) yields

$$S\tilde{m}_0 - \frac{\sqrt{1-q}}{\beta\varepsilon(\gamma-1)}\tilde{f} = -\frac{q}{2}\overline{m}\tilde{\theta}_{b1}. \tag{108}$$

Using (102) $\tilde{m}_0 = (\overline{m}+\kappa^+)\tilde{\theta}_{b1}/2$

$$S(\overline{m}+\kappa^+)\frac{\tilde{\theta}_{b1}}{2} - \frac{\sqrt{1-q}}{\beta\varepsilon(\gamma-1)}\tilde{f} = -q\overline{m}\,\frac{\tilde{\theta}_{b1}}{2}, \tag{109}$$

$$(S+q)\overline{m}\frac{\tilde{\theta}_{b1}}{2} - \frac{\sqrt{1-q}}{\beta\varepsilon(\gamma-1)}\tilde{f} = -S\kappa^+\frac{\tilde{\theta}_{b1}}{2}, \quad \kappa^+ \equiv \frac{\overline{m}}{2}\left[-1+\sqrt{1+4\mathrm{i}\omega/\overline{m}^2}\right]. \tag{110}$$

After substitution $\mathrm{i}\omega \to \sigma$, an equation for the linear growth rate σ (dispersion relation) is obtained when the expressions for $\tilde{\theta}_{b1}$ and $\tilde{m}_0$ in (105) are introduced into (110)

$$(S+q)\overline{m}\frac{(1-q)}{2} - \frac{\sqrt{1-q}}{\beta\varepsilon(\gamma-1)} = -(S+q)\overline{m}\,\frac{q}{2}\mathscr{Z}(\sigma) - S\frac{\overline{m}}{4}(\sqrt{1+4\sigma/\overline{m}^2}-1)[(1-q)+q\,\mathscr{Z}(\sigma)] \tag{111}$$

$$|\sigma| \ll 1: \quad \approx -\left[(S+q)\overline{m}\frac{q}{4} + S\frac{\overline{m}}{8}(1-q)\right]\frac{4}{\overline{m}^2}\sigma + O(\sigma^2)$$

$$\approx -\frac{1}{2\overline{m}}[S(1+q)+2q^2]\sigma = -\frac{\overline{m}}{2}(1-q)[S\Delta\tau_m + q\Delta\tau_\theta]\sigma. \tag{112}$$

The left-hand side of (112) is zero at the critical elongation and negative on the physical branch of the quasi-steady solutions as noticed by the derivative of (57) with respect to the pressure

$$(S+q)\mathrm{e}^{(1-q)\overline{f}/2} = (S_i+q) + \frac{\sqrt{1-q}}{\beta\varepsilon(\gamma-1)}\,\overline{f}, \quad f \equiv \beta\varepsilon[(\gamma-1)/\gamma]\pi_P, \quad \overline{m} = \mathrm{e}^{(1-q)\overline{f}/2} \tag{113}$$

$$\frac{\mathrm{d}S}{\mathrm{d}\overline{f}}\mathrm{e}^{(1-q)\overline{f}/2} = -(S+q)\mathrm{e}^{(1-q)\overline{f}/2}\frac{(1-q)}{2} + \frac{\sqrt{1-q}}{\beta\varepsilon(\gamma-1)}. \tag{114}$$

The physical branch being characterized by $\mathrm{d}S/\mathrm{d}\overline{f} > 0$, the left-hand side of (112) is negative so that this branch is unstable since the growth rate is positive $\sigma > 0$ and goes to zero on the turning point $\lim_{(S^*-S)\to 0^+}\sigma \to 0$, it should be for the exchange of stability between two branches of quasi-steady solutions merging on a turning point (saddle-node bifurcation).

To conclude this section, the physical branch of quasi-steady solutions associated with the back-flow (107) $\mathrm{v}_b = S\,m$ is unstable. The instability of the self-accelerating flame is inherent to the thermal feedback loop responsible for the turning point; the flame temperature increases with the pressure of the external flow which increases in turn with the laminar flame velocity and thus with the flame temperature.

6.3. *Stabilisation by unsteadiness effects in the burned gas flow*

The instability concerns flames subjected to a back-flow proportional to the laminar flame velocity $\mathrm{v}_b = S\mathrm{u}_b$ corresponding to a burned gas flow in quasi-steady state when the pressure varies while the unsteady effects have been retained in the cold flow ahead of the flame. A more consistent stability analysis should take into account the unsteadiness of the burned gas flow. Unfortunately the unsteady flow of burned gas in a finger flame is too complicated to be studied analytically. Hopefully a detailed study is not needed and a phenomenological modeling is sufficient to improve our understanding of the DDT.

6.3.1. *Delayed back-flow model*

Following [14], the longitudinal gradient of burned gas flow on the tube axis $u(\mathrm{x},t)$ is roughly modeled by a source term of mass whose origin is the burning of the lateral flame parallel to the wall. Denoting the laminar flame velocity (relative to the burned gas) of the lateral flame $U_{bw}(\mathrm{x},t)$, the gradient of the flow on the tube axis $u(\mathrm{x},t)$ is approximated by a one-dimensional mass conservation in a one-dimensional incompressible flow

$$\frac{\partial u}{\partial \mathrm{x}} = \frac{2}{R} U_{bw}(\mathrm{x},t) \tag{115}$$

where R is the radius of the tube. The longitudinal back-flow $u_b(t)$ impinging the tip from behind is obtained by integration along the tube axis. For a closed-end tube on the burned gas side, assuming an incompressible flow of burned gas at rest behind the foot of the finger-flame as in Figure 1, one gets

$$u_b(t) \equiv u(\mathrm{x}=\mathrm{X}_P(t),t) = \frac{2}{R}\int_{\mathrm{X}_P-L}^{X_P} U_{bw}(\mathrm{x},t)\mathrm{d}\mathrm{x} \tag{116}$$

where $\mathrm{X}_P(t)$ is the position of the tip and $L(t)$ the length of the elongated flame. The preceding model $u_b(t) = S(t)\,U_b(t)$ ($S = 2L/R$ in cylindrical geometry) is obtained by neglecting both heat loss on the wall and unsteadiness of the burned gas flow so that U_{bw} was considered as uniform along the lateral flame front and equal to the laminar flame velocity on the tip at the same time $U_{bw}(t) = U_b(t)$. Taking advantage of the planar approximation valid under the condition described in Section 3.2, the unsteady effects of the burned gas flow can be modeled by a delay $\Delta t(\mathrm{X}_P - \mathrm{x})$ introduced by the quasi-planar downstream-running compression waves between the state of the gas controlling the laminar flame velocity $U_b(t)$ on the tip at time t and on the lateral wall at a distance $X_P - \mathrm{x}$ from the tip $U_{bw}(\mathrm{x},t) \approx U_b(t-\Delta t(\mathrm{X}_P-\mathrm{x}))$,

$$u_b(t) \approx \frac{2}{R}\int_{\mathrm{X}_P-L}^{X_P} U_b(t-\Delta t(\mathrm{X}_P-\mathrm{x}))\mathrm{d}\mathrm{x}. \tag{117}$$

Assuming short delays compared to the characteristic time on the tip $U_b(t)$, $U_b/(\mathrm{d}U_b/\mathrm{d}t) \gg \Delta t(\mathrm{X}_P-\mathrm{x})$ and neglecting second order effects, a Taylor expansion yields

$$U_b(t-\Delta t) \approx U_b(t) + \Delta t\,\mathrm{d}U_b/\mathrm{d}t \quad \Rightarrow \quad u_b(t) \approx \frac{2L(t)}{R}U_b(t) - \frac{2}{R}\frac{\mathrm{d}U_b}{\mathrm{d}t}\int_{\mathrm{X}_P-L}^{X_P}\Delta t(\mathrm{X}_P-\mathrm{x})\mathrm{d}\mathrm{x}. \tag{118}$$

According to the downstream-running acoustic wave in the burned gas with a quasi-constant sound speed a_b, $\Delta t(\mathrm{X}_P-\mathrm{x})\approx(\mathrm{X}_P-\mathrm{x})/a$, $\Delta t_w\equiv\int_{\mathrm{X}_P-L}^{X_P}\Delta t(\mathrm{X}_P-\mathrm{x})\mathrm{d}x\approx L^2/2a_b$, Equation (118) yields, after introducing the overall delay Δt_w,

$$\text{delayed back-flow:}\quad u_b(t)\approx S(t)\left[U_b(t)-\Delta t_w\frac{\mathrm{d}U_b}{\mathrm{d}t}\right],\quad \Delta t_w\equiv\frac{L}{2a_b}. \tag{119}$$

It is worth stressing that, due to the thermal amplification by a large activation energy, the modification to u_b is mainly due to the change in burned gas flow U_b issued from the lateral flames, the effect of the flow velocity of the acoustic wave being negligible.

6.3.2. *Stability of the quasi-steady solutions*

The additional delay introduced by the delayed back-flow counteracts the unstable mechanism associated with the delays (103)–(104) introduced by the response of the inner flame structure. Introducing (119) written in non-dimensional form

$$\mathrm{v}_b(t)\approx\left[m_o-\Delta\tau_w\frac{\mathrm{d}m_o}{\mathrm{d}\tau}\right]S,\quad \tilde{\mathrm{v}}_b\approx(1-\Delta\tau_w\sigma)\tilde{m}_0(\sigma)S\quad \Delta\tau_w\approx\frac{L/t_{bi}}{2a_b}=\frac{\varepsilon}{2}\frac{L}{d} \tag{120}$$

into the linearized form (68) of the master equation yields the dispersion relation in the form

$$(1-\Delta\tau_w\sigma)\tilde{m}_0S-\frac{\sqrt{1-q}}{\beta\varepsilon(\gamma-1)}\tilde{f}=-\frac{q}{2}\overline{m}\tilde{\theta}_{b1} \tag{121}$$

where the linear expressions of $\tilde{\theta}_{b1}$ and $\tilde{m}_0$ proportional to $\tilde{f}$ are given by the response to pressure fluctuations in (103) and (104). Equation (121) which differs from (108) by the term $-\Delta\tau_w\tilde{m}_0S\sigma=-\Delta\tau_w\overline{m}(1-q)S\sigma/2+O(\sigma^2)$ yields

$$|\sigma|\ll1:\quad (S+q)\overline{m}\frac{(1-q)}{2}-\frac{\sqrt{1-q}}{\beta\varepsilon(\gamma-1)}=-\frac{\overline{m}}{2}(1-q)[S(\Delta\tau_m-\Delta\tau_w)+q\Delta\tau_\theta]\sigma+O(\sigma^2) \tag{122}$$

instead of (112). Using the same arguments as in the text below (112), Equation (122) shows that the physical branch is stable under the condition

$$\Delta\tau_w>\Delta\tau_m+(q/S)\Delta\tau_\theta\Leftrightarrow\varepsilon\frac{L}{d}>\frac{2}{(1-q)\overline{m}^2}\left[(1+q)+\frac{2q}{S}\right] \tag{123}$$

which is easily fulfilled under the condition (8) for the validity of the asymptotic analysis in the limit (6) since the parameter $2[(1+q)+2q/S]/[(1-q)\overline{m}^2]$ is of order unity, see the text below (7). Moreover the linear growth rate still vanishes at the critical condition and changes sign on the nonphysical branch branch $\overline{\vartheta}_+(\zeta)$ which becomes unstable as it should be, see Figure 1.

7. Nonlinear dynamics. Dynamical saddle-node bifurcation

The nonlinear dynamics takes the form of a differential equation for the pressure on the flame $1+\varepsilon\pi_P(\tau)$ obtained by the asymptotic analysis of the unsteady flame structure leading to the master equation (49) linking the velocity jump across the flame structure u_b-u_u to the instantaneous flame temperature $T_b(t)$, see Figure 2. Using the notation $\theta_{b1}\equiv\beta[T_b(\tau)-T_b(0)]/T_b(0)=O(1)$ and the delayed back-flow (120) one gets

$$\left[m_o(\pi_P)-\Delta\tau_w\frac{\mathrm{d}m_o}{\mathrm{d}\tau}\right](1+\epsilon\tau)S_i-\left[S_i+q+\frac{\sqrt{1-q}}{\gamma}\pi_P(\tau)\right]=-q\mathrm{e}^{\theta_{b1}(\pi_P)/2}+O(\varepsilon), \tag{124}$$

where the first and the second term on the left-hand side are respectively the instantaneous back-flow $u_b(t)$ and the flow velocity just ahead of the flame $u_u(t)$ as it is modified from its initial value $\pi_P(0)=0$, $u_u(0)=S_i+q$ by the downstream running compression waves in the external flow ahead of the flame, see (44) and Figure 2. For a weakly perturbed inner structure of the flame, the flame temperature $\theta_{b1}(\pi_P)$ and the laminar flame velocity $m_o(\pi_P)$, expressed in terms of the

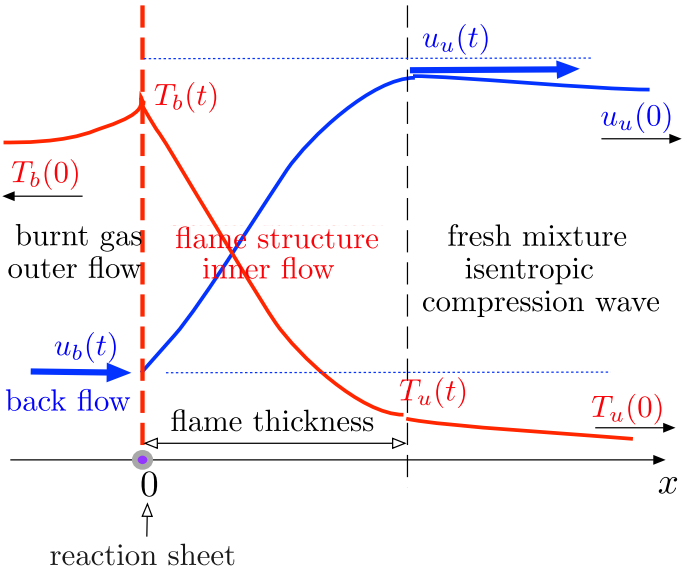

Figure 2. Sketch of the unsteady flame structure in the framework of the reaction sheet ($x = 0$). The problem being hyperbolic, the boundary condition at $x \to \pm\infty$ is the initial condition in the burned and unburned gas, $\lim_{x\to-\infty} u_b(t) = u_b(0)$ and $\lim_{x\to+\infty} u_u(t) = u_u(0)$ respectively.

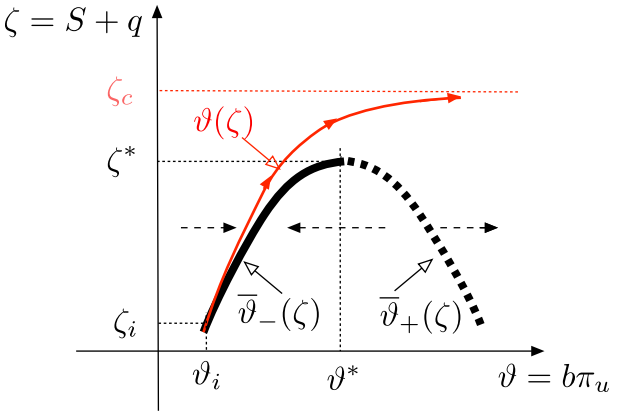

Figure 3. Sketch of the solutions "elongation ζ versus pressure ϑ" (not to scale). The two branches $\overline{\vartheta}_\pm(\zeta)$ of the quasi-steady solutions of (60) $\zeta = F(\vartheta)$ in thick line show the critical elongation ζ^*, above which there is no quasi-steady solutions (saddle-node bifurcation); $\overline{\vartheta}_-$ in solid line is the physical solution which is stable under the condition (123). The thin red curve represents the finite-time singularity of the solution of the dynamical equation in (134). The sudden increase in pressure and flame temperature ϑ leads to a spontaneous DDT at finite time for an elongation $\zeta = \zeta_c$ slightly larger than the critical elongation ζ^*.

instantaneous flame pressure $\pi_P(t)$, to be introduced into (124), are given by the linear response of the flame to pressure fluctuations studied in Section 6.1.

7.1. *Nonlinear dynamics for a quasi-steady inner structure of the flame*

To enlighten the essential features of the nonlinear dynamics nearby the critical conditions, it is worth starting by assuming a quasi-steady inner structure of the flame so that the expressions of $\theta_{b1}/2$ and m_o in terms of π_P are the same as (55) for the steady-state solution $\theta_{b1}/2 = b\pi_P$, $m_o = \mathrm{e}^{b\pi_P}$ yielding $\mathrm{d}m_o/\mathrm{d}\tau = \mathrm{e}^{b\pi_P} b\mathrm{d}\pi_P/\mathrm{d}\tau$. Introducing these expressions into (124) yields

$$\left[S_i(1+\epsilon\tau)+q\right]\mathrm{e}^{b\pi_P(\tau)} - \left[S_i + q + \frac{\sqrt{1-q}}{\gamma}\pi_P(\tau)\right] = (1+\epsilon\tau)S_i\Delta\tau_w \mathrm{e}^{b\pi_P}\, b\,\frac{\mathrm{d}\pi_P(\tau)}{\mathrm{d}\tau}. \qquad (125)$$

The term on the right-hand side is the dynamical effect of the unsteadiness of the downstream running compression waves in the burned gas, leading to the delay $\Delta\tau_w > 0$ in the back-flow. If this delay is neglected $\Delta\tau_w = 0$, Equation (125) reduces to the nonlinear equation for the quasi-steady solutions characterized by a turning point. Using the same notation as in (58)–(59), $\vartheta \equiv b\pi_P$ for the pressure (or the flame temperature when the flame structure is in steady state), $\zeta \equiv (1+\epsilon\tau)S_i + q$ for the elongation (or the time since the time derivative $\mathrm{d}\zeta/\mathrm{d}\tau = \epsilon S_i$ is a constant) and a parameter of order unity $\mathrm{b} \equiv (\beta\varepsilon/2)(\gamma-1)\sqrt{1-q}$, Equation (125), after simplification by e^{ϑ}, takes the form of a non-autonomous (and nonlinear) ordinary differential equation for $\vartheta(\zeta)$, namely the function "pressure versus elongation",

$$\zeta - \left[\zeta_i + \frac{\vartheta}{\mathrm{b}}\right]\mathrm{e}^{-\vartheta} = \epsilon(1+\epsilon\tau)S_i^2\Delta\tau_w\frac{\mathrm{d}\vartheta}{\mathrm{d}\zeta}. \qquad (126)$$

For clarity it is worth introducing the function $F(\vartheta) = [\zeta_i + \vartheta/\mathrm{b}]\,\mathrm{e}^{-\vartheta}$ which presents a maximum at the critical point $\zeta^* = (1/\mathrm{b})\mathrm{e}^{-\vartheta^*}$, $\vartheta^* = 1-\zeta_i\mathrm{b}$, see (61). Neglecting terms of order ϵ^2, Equation (126) can then be written

$$\zeta - F(\vartheta) = \epsilon S_i^2\Delta\tau_w\frac{\mathrm{d}\vartheta}{\mathrm{d}\zeta}. \qquad (127)$$

The quasi-steady solutions $\overline{\vartheta}(\zeta)$ are represented by the two real roots of the left-hand side of (127) $\zeta = F(\overline{\vartheta})$ that exist for $\zeta \leqslant \zeta^*$. The two branches $\overline{\vartheta}_\pm(\zeta)$ merge at $\zeta = \zeta^*$ and disappear for $\zeta > \zeta^*$, see Figure 3 and the text below (61). The physical branch of the quasi-steady solutions is $\overline{\vartheta}_-(\zeta) \leqslant \vartheta^*$ for which $\mathrm{d}\overline{\vartheta}_-/\mathrm{d}\zeta > 0$. The solution of (127) around a point (ϑ_o, ζ_o) on the physical branch of quasi-steady solutions $\zeta_o = F(\vartheta_o)$ is obtained by a power expansion in the form $\delta\vartheta = \vartheta - \vartheta_o$, $\delta\zeta = \zeta - \zeta_o$

$$\delta\zeta - \delta\vartheta\left.\frac{\partial F}{\partial\vartheta}\right|_{\vartheta=\vartheta_o} - \frac{1}{2}(\delta\vartheta)^2\left.\frac{\partial^2 F}{\partial\vartheta^2}\right|_{\vartheta=\vartheta_o} = \epsilon S_i^2\Delta\tau_w\frac{\mathrm{d}\delta\vartheta}{\mathrm{d}\delta\zeta}, \qquad (128)$$

where $\vartheta_o < \vartheta^* : \partial F/\partial\vartheta|_{\vartheta=\vartheta_o} > 0$ and $\partial F/\partial\vartheta|_{\vartheta=\vartheta^*} = 0$, $\partial^2 F/\partial\vartheta^2|_{\vartheta=\vartheta^*} = -\zeta^* < 0$. The two first terms on the left-hand side of (128) represent the linear dynamics of the quasi-steady solutions on the physical branch. The stability of the steady solution at $\zeta = \zeta_0$ on the physical branch is obtained from the second term on the left-hand side using $\delta\zeta = 0$ in the first term. For a positive delay $\Delta\tau_w > 0$ introduced by the downstream running acoustic waves in the burned gas, the physical branch of quasi-steady solutions $\overline{\vartheta}_-(\zeta) \leqslant \zeta^*$ is stable, $\mathrm{d}F/\mathrm{d}\zeta > 0$. The third term on the left-hand side of (128) becomes dominant near the critical point $\partial F/\partial\vartheta|_{\vartheta=\vartheta^*} = 0$ indicating how the critical dynamics is strongly modified by the nonlinear feedback loop of temperature in the compressible flow ahead of the flame. Focusing the attention on the vicinity of the critical point $\delta\vartheta = \vartheta - \vartheta^*$, $\delta\zeta = \zeta - \zeta^*$, the second term on the left-hand side of (128) vanishes and we are left with

$$\frac{\zeta-\zeta^*}{\zeta^*} + \frac{1}{2}(\vartheta-\vartheta^*)^2 = \tilde{\epsilon}\frac{\mathrm{d}(\vartheta-\theta^*)}{\mathrm{d}(\zeta/\zeta^*)} \quad \text{where } \tilde{\epsilon} = \epsilon\frac{S_i^2}{\zeta^{*2}}\Delta\tau_w > 0. \qquad (129)$$

The two roots of the left-hand side $\zeta < \zeta^*$: $\overline{\vartheta}_\pm = \vartheta^* \pm \sqrt{2(\zeta^*-\zeta)/\zeta^*}$ are the quasi-steady solutions (flame pressure or temperature versus elongation) resulting from the compressional heating by the downstream running compression waves in the unburned gas ahead of the flame that are

generated by the back-flow without delay, $u_b = S(\tau)U_b(\tau)$. However, the dynamics is drastically modified near the critical condition by the quadratic term on the left-hand side of (129). Generally speaking, Equation (129) describes the dynamics nearby a saddle-node bifurcation and was extensively used for sharp transitions in different problems of physics or biophysics.

7.2. *Dynamical saddle-node bifurcation*

Conveniently rescaled

$$(1/2^{2/3})(1/\tilde{\epsilon})^{1/3}(\vartheta-\vartheta^*)\to y',\quad (1/2^{1/3})(1/\tilde{\epsilon})^{2/3}(\zeta-\zeta^*)/\zeta^*\to t', \tag{130}$$

Equation (129) takes, after multiplication by $(1/\sqrt{2}\tilde{\epsilon})^{2/3}$, the generic normal form

$$\frac{\mathrm{d}y'(t')}{\mathrm{d}t'} = t' + y'^2 \tag{131}$$

which was extensively used in the theory of catastrophic events recently revisited and extended in [21]. For $t'<0$, the solution of (131) has two fixed points collapsing at $t'=0$, the stable one corresponding to the negative root $y'=-\sqrt{-t'}$ (physical branch of solutions). Considering an initial condition on the stable branch $t'=t'_i<0: y'=-\sqrt{-t'_i}$ for $-t'_i/t'_c = y'^2_i/t'_c$ large enough, the asymptotic solution of (131) is obtained in terms of the Airy function to give

$$\lim_{t'\to t'_c} y'(t') = \frac{1}{t'_c-t'} - \frac{t'_c}{3}(t'_c-t') + \cdots \quad \text{where } t'_c \approx 2.338\ldots, \tag{132}$$

see the references in [21]. The finite-time singularity of the solutions to (132) is of the same type as obtained with the Riccati equation $\mathrm{d}y'/\mathrm{d}t' = y'^2$. The pressure and flame temperature $\vartheta \equiv b\pi_P(\tau)$ blow up at finite time $\tau=\tau_c$ for a finite elongation $\zeta_c = S_i(1+\epsilon\tau_c)+q$, $(\zeta_c-\zeta^*) = (\tau_c-\tau^*)\epsilon S_i$

$$\frac{(\zeta_c-\zeta^*)/\zeta^*}{(2\tilde{\epsilon}^2)^{1/3}} = 2.338\ldots, \quad b(\pi_u-\pi_u^*) \equiv \vartheta-\vartheta^* \approx 2\tilde{\epsilon}\frac{\zeta^*}{\zeta_c-\zeta} = 2\frac{S_i}{\zeta^*}\frac{\Delta\tau_w}{\tau_c-\tau}. \tag{133}$$

The solution $\vartheta(\tau)$ still exists above the critical elongation ζ^* and diverges at $\zeta=\zeta_c>\zeta^*$ $(\tau_c>\tau^*)$ like $\Delta\tau_w/(\tau_c-\tau)$ where $\tau_c-\tau^*\propto 1/\epsilon^{1/3}$, see Figure 3. The smaller the elongation rate ϵ, the closer to the critical elongation S^* the divergence of the pressure, $\lim_{\epsilon\to 0}(S_c-S^*)/S^*\propto\epsilon^{2/3}$. In contrast to Section 5.2 where the compression waves in the burned gas are neglected ($\Delta\tau_w=0$) a violent increase in pressure and flame temperature develops suddenly for an elongation $S=S_c$ slightly larger than S^*. The existence of a finite-time singularity is not limited to the quadratic expansion on the left-hand side of (129); a similar singularity is exhibited by the solution of (126) which is not limited to small values of $|\vartheta-\vartheta^*|$.

Notice that Equation (129) for $\tilde{\epsilon}<0$ would lead to $-\mathrm{d}y'(t')\mathrm{d}t' = t'+y'^2$ showing that the stable branch would be $y'=\sqrt{-t'}$ and the finite-time singularity would correspond to $\lim_{t'\to t'_c} y' = -\infty$. Therefore the sign $\tilde{\epsilon}>0$ in (129) is essential for relevant physical insights into the DDT of self-accelerated laminar flames in tubes.

7.3. *Effects of the unsteadiness of the inner structure of the flame*

A small unsteadiness of the inner structure of the flame does not modify qualitatively the nonlinear dynamics provided the quasi-steady solutions are stable. Considering a characteristic time scale of the dynamics larger than the transit time t_b (slow dynamics generated by a slow increase in elongation (5) for $\epsilon\ll 1$), the disturbances of the flame temperature and of the laminar flame velocity due to the time derivative of the pressure on the right-hand side of (38) (energy conservation) are accurately modeled by the linear expressions (103)–(104). Introducing the latter into (124) and following the same development as in Section 6.3.2 one gets neglecting ϵ^2-terms

$$\zeta - F(\vartheta) = \epsilon S_i^2\left(\Delta\tau_w - \Delta\tau_m - \frac{q}{S_i}\Delta\tau_\theta\right)\frac{\mathrm{d}\vartheta}{\mathrm{d}\zeta} \tag{134}$$

leading to the same equation as (129) but with a different expression for $\tilde{\epsilon}$

$$\tilde{\epsilon} = \epsilon \frac{S_i^2}{\zeta^{*2}} \left(\Delta\tau_w - \Delta\tau_m - \frac{q}{S_i} \Delta\tau_\theta \right) \tag{135}$$

where $\tilde{\epsilon} > 0$ in the stable case, see Section 6.3.2. The results presented in the preceding section are still valid ($\Delta\tau_w \to \Delta\tau_w - \Delta\tau_m - q\Delta\tau_\theta / S_i > 0$) as long as $\tilde{\epsilon} \mathrm{d}\vartheta/\mathrm{d}\zeta$ remains not much smaller than unity that is until the slope $\mathrm{d}\zeta/\mathrm{d}\vartheta$ of the curve in red in Figure 3 is larger than $\tilde{\epsilon}$. According to (133), this is the case for $\zeta_c - \zeta > \tilde{\epsilon}$, namely until a time τ relatively close to τ_c, $(\tau_c - \tau) \approx \tilde{\epsilon}^{1/3}(\tau_c - \tau^*)$ for which the relative increase in flame temperature is of order unity $(\vartheta - \vartheta^*)/\vartheta^* = O(1)$. However the results of Section 7.2 are no longer accurate for $(\vartheta - \vartheta^*)/\vartheta^* > 1$ because of the break down of the slow timescale assumption used in (103)–(104).

However, the existence of a finite-time singularity is not doubtful, as discussed in the next section. A simple explanation can be given for the finite time singularity sketched by the red curve in Figure 3. The generic divergence of the flame acceleration in the quasi-steady solutions $\overline{\vartheta}_-(\zeta)$ at the bifurcation $\zeta = \zeta^*$, $\mathrm{d}\vartheta_-/\mathrm{d}\zeta|_{\zeta=\zeta^*} = \infty$ is delayed to $\zeta = \zeta_c > \zeta^*$ by the delay $\Delta\tau_w$ of the back-flow appearing on the left-hand side of (124) and the solution $\vartheta(\zeta)$ must go to infinity since there is no steady state solution above ζ^* but the expression (133) of ζ_c, obtained with the quadratic approximation, may not be accurate. The singularity is thus expected to appear systematically whatever the elongation rate and the delay in the back-flow, as small as they may be.

8. Discussion of the results and conclusion

The nonlinear dynamics of the one-dimensional model for a self-accelerated flame on the tip of an elongated flame front has been investigated in the double limit of large activation energy and small Mach number of laminar flames. Starting with a small growth rate of elongation from a self-similar solution (constant elongation), the downstream running compressible waves coupled with the quasi-isobaric flame produces a sudden transition. The role of the compressible waves is different in the unburned and burned gas flows. In the unburned gas, the flame acts as an accelerating semi-transparent piston and the compressional heating produces a nonlinear thermal feed back loop responsible for a saddle-node bifurcation similar to that characterizing the self-similar solutions. The compressible waves in the burned gas flow introduce unsteadiness in the back-flow. The latter is the mechanism through which the flame on the tip is accelerated when the elongation of the finger like front increases (increase in surface area of the finger-shaped flame front). The joined effect of these two unsteady mechanisms lead to a finite-time singularity of the flame temperature and pressure in the form of a saddle-node bifurcation.

This was proved in a first step, assuming a flame structure in steady state. Clearly, the assumption of a inner structure of the flame in quasi-steady state is no longer valid as soon as the timescale of the dynamics becomes smaller than the transit time across the laminar flame structure as it is the case for a finite-time singularity of the flame temperature. When the flames associated with a constant elongation are stable against pressure disturbances, the qualitative feature of the finite-time singularity is shown by a perturbation analysis to not be modified by the unsteadiness of the inner structure. This analysis is valid until the slow time scale assumption in the dynamics of the inner structure of the flame breaks down in the ultimate divergence of the flame temperature and pressure. In addition to the comment at the end of Section 7.3, there are two other good reasons to conjecture that a finite-time singularity characterizes effectively the unsteady inner solution of the reactive flow of a self-accelerated laminar flame: firstly, flame quenching cannot occur with an increase in flame temperature, secondly there is no other combustion waves in a one-dimensional geometry than laminar flames and detonations. Nevertheless, transient regimes similar to intermittent quenching and re-ignition of the detonation

cannot be completely ruled out, even though they are not likely in the absence of oscillatory flames (unity Lewis number) and galloping detonations. Some work remains to be done in this direction.

A strong shock should be generated by the pressure runaway leading quasi-instantaneously to the DDT onset. The pre-conditioned state of unburned gas just ahead of the flame and just before the abrupt transition is characterized by a universal critical Mach number of the induced flow of unburned gas which is close to unity, in agreements with experiments and direct numerical simulations. This critical condition is all the easier to achieve in very energetic mixtures for an elongation which is not so large. This could well be the case for the cellular structure of Rayleigh–Taylor unstable flame fronts of very energetic mixtures as those involved in supernovae SNIa. On the contrary, the transition to detonation of laminar flames in tubes filled with weakly energetic mixtures is not possible because the predicted critical elongation is too large to be observed.

To summarize, the DDT mechanism presented in this article concerns the one-dimensional dynamics of reacting flows characterized by a rate of heat release highly sensitive to the temperature. Although the origin of the self-induced flow responsible for the flame acceleration is multi-dimensional (increase in surface area of the elongated flame front), the DDT onset is a local process of a one-dimensional nature. This mechanism of transition concerns also turbulent wrinkled flames and/or unconfined cellular flames, the flame brush being considered as a chaotic array of elongated flames the tip of which is accelerated by the self-induced flow associated with an increase in surface area of the wrinkled flame front. In that sense, the DDT mechanism described here could have a certain degree of universality. This should be confirmed by direct numerical simulations.

Declaration of interests

The authors do not work for, advise, own shares in, or receive funds from any organization that could benefit from this article, and have declared no affiliations other than their research organizations.

Acknowledgments

Yves Pomeau is acknowledged for enlightening discussion on the dynamical saddle-node bifurcation. I am grateful to Grisha Sivashinsky for drawing my attention few years ago on the work of Joulin and Deshaies. I thank Misha Liberman for fruitful discussions on DDT and comments on the manuscript. I thank also Professors Bruno Denet, Guido Lodato, Luc Vervisch and the Phd students Raúl Hernández-Sánchez and Hassan Tofaili for lively interactions during their numerical activities. Partial financial support of *Agence National de la Recherche* (contract ANR-18-CE05-0030) is acknowledged.

References

[1] K. I. Shchelkin, Yu. K. Troshin, *Gasdynamics of Combustion*, Mono Book Corp., Baltimore, 1965.
[2] J. Lee, *The Detonation Phenomenon*, Cambridge University Press, Cambridge, 2008.
[3] P. Clavin, G. Searby, *Combustion Waves and Fronts in Flows*, Cambridge University Press, Cambridge, 2016.
[4] P. Clavin, "One-dimensional mechanism of deflagration-to-detonation in gas", *J. Fluid. Mech.* **974** (2023), article no. A46.
[5] A. Sanchez, F. A. Williams, "Recent advances in understanding of flammability characteristics of hydrogen", *Prog. Energy Combust. Sci.* **41** (2014), p. 1-55.
[6] P. Clavin, H. Tofaili, "A one-dimensional model for deflagration-to-detonation transition on the tip of elongated flames in tubes", *Combust. Flame* **232** (2021), article no. 111521.

[7] Ya. B. Zeldovich, D. A. Frank-Kamenetskii, "A theory of thermal flame propagation", *Acta Phys. Chim.* **9** (1938), p. 341-350.
[8] M.-H. Wu, C.-Y. Wang, "Reaction propagation modes in millimeter-scale tubes for ethylene/oxygen mixtures", *Proc. Combust. Inst.* **33** (2011), p. 2287-2293.
[9] V. Bykov, A. Koksharov, M. Kuzetsov, V. P. Zhukov, "Hydrogen-oxygen flame acceleration in narrow open ended channels", *Combust. Flame* **238** (2022), article no. 111913.
[10] P. A. Urtiew, A. K. Oppenheim, "Experimental observations of the transition to detonation in an explosive gas", *Proc. R. Soc. Lond. A* **295** (1966), p. 13-28.
[11] M. A. Liberman, M. F. Ivanov, A. D. Kiverin, M. S. Kuznetsov, A. A. Chukalovsky, T. V. Rakhimova, "Deflagration-to-detonation transition in highly reactive combustion mixtures", *Acta Astronaut.* **67** (2010), p. 688-701.
[12] M. Kuznetsov, M. Liberman, I. Matsukov, "Experimental study of the preheated zone formation and deflagration to detonation transition", *Combust. Sci. Tech.* **182** (2010), p. 1628-1644.
[13] Ya. B. Zeldovich, "Regime classification of an exothermic reaction with nonuniform initial condition", *Combust. Flame* **39** (1980), p. 211-214.
[14] C. Clanet, G. Searby, "On the tulip flame phenomenon", *Combust. Flame* **105** (1996), p. 225-238.
[15] B. Deshaies, G. Joulin, "Flame-speed sensitivity to temperature changes and the deflagration-to-detonation transition", *Combust. Flame* **77** (1989), p. 202-212.
[16] L. Kagan, G. Sivashinsky, "Parametric transition from deflagration to detonation: Runaway of fast flames", *Proc. Combust. Inst.* **36** (2017), p. 2709-2715.
[17] P. Clavin, M. Champion, "Asymptotic solutions of two fundamental problems in gaseous detonations", *Combust. Sci. Technol.* **195** (2023), no. 15, p. 3663-3694.
[18] P. Clavin, "Finite-time singularity associated with the deflagration-to-detonation transition on the tip of an elongated flame-front in a tube", *Combust. Flame* **245** (2022), article no. 112347.
[19] P. Clavin, P. Pelcé, L. He, "One-dimensional vibratory instability of planar flames propagating in tubes", *J. Fluid Mech.* **216** (1990), p. 299-322.
[20] G. Joulin, P. Clavin, "Linear stability analysis of non adiabatic flames: Diffusional-thermal model", *Combust. Flame* **35** (1979), p. 139-153.
[21] R. D. Peters, M. Le Berre, Y. Pomeau, "Prediction of catastrophes: a experimental model", *Phys. Rev. E* **86** (2012), article no. 026207.